Design of Machines and Structures, Vol. 14, No. 1 (2024), pp. 5–12.
https://doi.org/10.32972/dms.2024.001

ADDITIVE MANUFACTURING FROM BIOMIMETIC APPROACH

JUDIT ALBERT[1] – ÁGNES TAKÁCS[2]

University of Miskolc, Institute of Machine and Product Design
H-3515, Miskolc-Egyetemváros
[1]szalai.judit@student.uni-miskolc.hu, [2]takacs.agnes@uni-miskolc.hu
[1]https://orcid.org/0000-0001-8043-5503, [2]https://orcid.org/0000-0002-3210-6964

Abstract: During the past millions of years since the beginning of our world, nature has created structures that are resistant to the various effects of the environment. However, these natural structures are quite complicated, so their production and artificial reproducibility with the tools of traditional manufacturing technology is a very difficult task. However, even complex structures can be produced relatively easily with the help of additive manufacturing. Using topological optimization techniques, lattice structure models with excellent mechanical characteristics can be created, which can be easily manufactured by exploiting the advantages of additive manufacturing. Applying natural structures (biomimetic approach) during topological optimization and produce the solution by additive manufacturing, light and high-strength structural alternatives can be created, any further structural analyses can be done.

Keywords: *additive manufacturing, lattice structures, biomimicry*

1. INTRODUCTION

The recent development of additive manufacturing (AM) techniques makes it possible to manufacture components with complex structures that cannot be produced with traditional manufacturing methods. Nowadays, when sustainability is gaining more and more importance, additive manufacturing also brings advantages such as shortening the production of the component, reducing energy consumption, and minimizing material waste (Tao & Leu, 2016) (Datta, Vyas, Dhara, Chowdhury, & Barui, 2019) (Plocher & Panesar, 2019) (Hoang, Tran, Vu, & Nguyen-Xuan, 2020). This method offers a new perspective to designers and engineers who use additive manufacturing during their work.
The study presents the relevance of lattice structures and topological optimization (Szabó, 2022) in a biomimetic approach, and also mentions the optimization of

lattice structures and the relationship between these methods and biomimetic. Fatigue tests are important for examining the fatigue behaviour, but they can only describe the correlations of the topology's fatigue properties phenomenologically. Since the stress distribution within the structure cannot be determined directly by fatigue tests, fatigue tests are also taking a lot of time and work if a large number of samples are used; so its efficiency is not high enough. (Huang, Wang, & Fan, 2023) Due to the limitations mentioned above, fatigue tests must be used in conjunction with other technologies to gain a comprehensive understanding of fatigue behaviour.

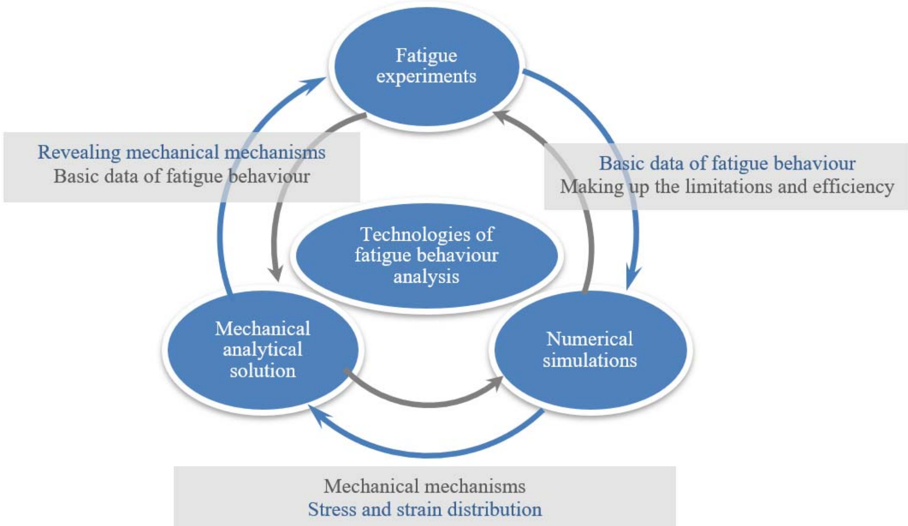

Figure 1. *Analysing methods of fatigue behaviour (Huang, Wang, & Fan, 2023)*

Most traditional manufacturing methods cannot provide the design freedom that AM does, thanks to which theoretical considerations, analytical solutions and computational models are used during design to establish so-called "design-property" relationships, which can be used to predict what topological design is required to achieve a given combination of desired properties. (Alzyod & Ficzere, 2023), (Alzyod, Borbas, & Ficzere, 2023) This often results so complex topological designs that can only be realized with advanced AM techniques.

2. LATTICE STRUCTURES

The development of additive manufacturing techniques has liberated the design of lattice structures by enabling the manufacturability of lattice structures (Voicu, Hadăr, & Vlăs, 2021). Lattice structures are primarily made up of nodes and stiffening elements, which significantly contribute to reducing mass and at the same time maintaining structural integrity (Gibson & Ashby, 1997), (Seharing, Azman, & Abdullah, 2020).

2.1. Mechanical properties of lattice structures

Since the properties of lattice structures depend directly on the shape and structure of the unit cell, each unit cell has different mechanical properties (Libonati, Graziosi, Ballo, Mognato, & Sala, 2023).

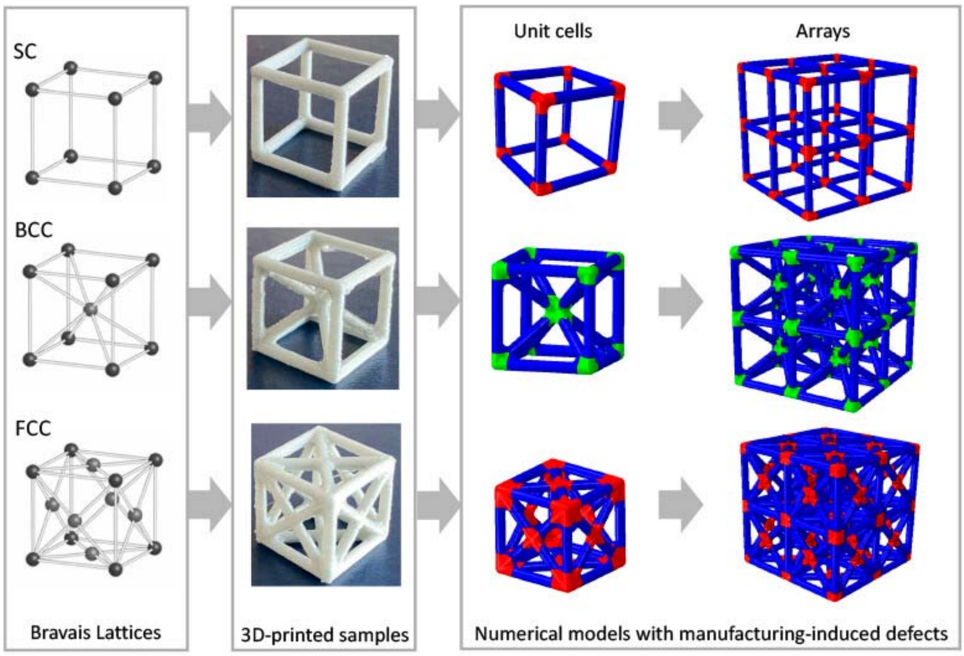

Figure 2. *Examples for building up lattice structures and unit cells (Libonati, Graziosi, Ballo, Mognato, & Sala, 2023)*

2.2. Advantages and disadvantages of grids

Traditionally, lattice structures can be made by casting and sheet forming, however, the manufacturing limitations of these methods greatly affect the complexity of the designed lattice structures. Therefore, with these methods, only a few lattice structures with a simple unit cell topology can be produced, in contrast to the possibilities of AM. The most important challenge for the designer in a construction is the selection of the appropriate variables. The material of the lattice, the cell type and the volume ratio play an important role in determining the structural stiffness and strength. The same applies to other mechanical properties. Since the size affects the mechanical performance, the mechanical characteristics of lattice structures, the smaller the relative density, the greater the size effect (Kladovasilakis, Tsongas, & Tzetzis, 2020).

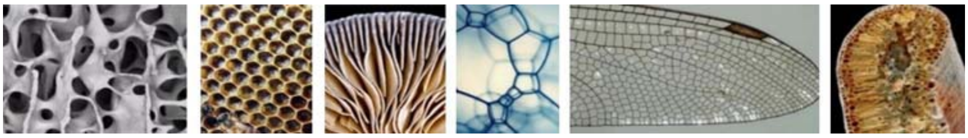

a) b) c) d) e) f)

Figure 3. *Lattice structure examples in nature*
a) microscopic photon of human bone, b) honeycomb structure, c) fungal mycelium, d) Voronoi structure in bubbles, e) wing of a dragonfly, f) cross section structure of a leaf (Nazir, Abate, Kumar, & Jeng, 2019)

2.3. Manufacturing lattice structures

The development of additive manufacturing techniques, such as 3D printing, has made it possible to create more complex structures when designing lattice structures. Thus, lattices created by AM methods can mimic biomaterials such as bone (Briguiet & Egan, 2020). While 2D extruded fabric-like gratings can be produced by conventional manufacturing methods such as casting, forging, and extrusion, 3D shell/sheet structures can be produced by the AM method, as it enables even complex structural structures to be produced (Nguyen, 2019).

3. Biomimicry

Ideas derived from the biological structures of nature's optimized complex structures have spread widely in the field of additive manufacturing thanks to the latest developments. These structures, which occur frequently in nature, are a source of inspiration for the design of various cell structures that can be used in engineering applications (du Plessis, et al., 2019), (Dömötör, 2005), (Dömötör & Péter, 2012), (Dömötör, 2014). Natural structures are often complex systems of several repeating structural elements. These biological structures can be listed as filamentous, helical, gradient, layered, tubular, cellular, sutural, and overlapping structures, as shown in Figure 3. Nature offers many effective solutions, e.g.: mineralized tubular skeletons from one such species, Euplectella aspergillum (Fernandes, et al., 2021) show very high strength, which results from the hierarchical arrangement of the porous light structure and different geometric structures.

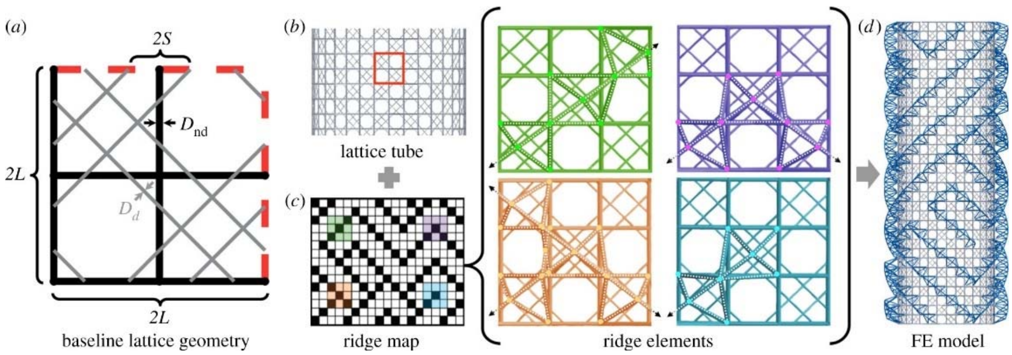

***Figure 4.** Workflow for creating structural models of Euplectella aspergillum:*

(a) schematic drawing of diagonally reinforced square unit cell geometry, to create the tubular grid shown in the figure (b), then (c) mapping of the schemes that make up the different elements used to create the complete lattice structure, and finally (d) modelling the pattern of the FEM model (Fernandes, et al., 2021)

The complex structures found in nature exceed conventional design and manufacturing technologies, hindering the progress of biomimetic studies and their use in engineering applications. AM has created new possibilities for the production of multifunctional structures made of several materials, and the integration of biomimicry will enable breakthroughs in the development of engineering technology in the coming decades (Yang, et al., 2018).

4. CONCLUSION

The mechanisms of natural synthesis need to be further studied to design usable bio-inspired structures in engineering systems. For this, AM manufacturing must be developed together with other technologies so that the mechanisms behind the properties of manufactured parts and the phenomena observed in nature can be explored. It is also important to understand and identify the growth processes that shape matter in nature, which can inspire the search for alternative methods to mimic the natural growth process on a shorter time scale. This way, 3D printing can best approach the growth process and at the same time meet the production timescale in an engineering environment. By understanding these materials and structures, research can provide further insight into methods for replicating these natural structures rather than simply replicating biological structures.

REFERENCES

Alzyod, H., & Ficzere, P. (2023). Material-Dependent Effect of Common Printing Parameters on Residual Stress and Warpage Deformation in 3D Printing: A Cromprehensive Finite Element Analysis Study. *Polymers, 15*(13). doi:https://doi.org/10.3390/polym15132893

Alzyod, H., Borbas, L., & Ficzere, P. (2023). Rapid prediction and optimization of the impact of printing parameters on the residual stress of FDM-ABS parts using L27 orthogonal array design and FEA. *Materials Today: Proceedings, 93*, 583-588. doi:https://doi.org/10.1016/j.matpr.2023.02.213

Briguiet, G., & Egan, P. (2020). Structure, Process, and Material Influences for 3D Printed Lattices Designed With Mixed Unit Cells. *ASME 2020 International Design Engineering Technical Conferences and Computers and Information in Engineering Conference.* Virtual, online. doi:https://doi.org/10.1115/DETC2020-22575

Datta, P., Vyas, V., Dhara, S., Chowdhury, A., & Barui, A. (2019). Anisotropy properties of tissues: a basis for fabrication of biomimetic anisotropic scaffolds for tissue engineering. *Journal of Bionic Engineering, 16*, 842-868. doi:https://doi.org/10.1007/s42235-019-0101-9

Dömötör, C. (2005). Natural motivations in engineering design. *GÉP, 56*, 25-26.

Dömötör, C. (2014). A természeti intuíció hatása a termékfejlesztés gyakorlatára. *GÉP, 65*(14), 23-36.

Dömötör, C., & Péter, J. (2012). Természeti elvek az analógia alapú tervezésben. *GÉP, 63*(12), 29-32.

du Plessis, A., Broeckhoven, C., Yadroitsava, I., Yadroitsev, I., Hands, C., Kunju, R., & Bhate, D. (2019). Beautiful and Functional: A Review of Biomimetic Design in Additive Manufacturing. *Additive Manufacturing, 27*, 408-427. doi:https://doi.org/10.1016/j.addma.2019.03.033

Fernandes, M., Saadat, M., Cauchy-Dubois, P., Inamura, C., Sirota, T., Milliron, G., . . . Weaver, J. (2021). Mechanical and hydrodynamic analyses of helical strake-like ridges in a glass sponge. *Journal of the Royal Society Interface, 18*(182). doi:https://doi.org/10.1098/rsif.2021.0559

Gibson, L., & Ashby, M. (1997). *Cellular Solids: Structure and Properties.* Cambridge: Cambridge University Press.

Hoang, V., Tran, P., Vu, V., & Nguyen-Xuan, H. (2020). Design of lattice structures with direct multiscale topology optimization. *Composite Structures, 252*. doi:https://doi.org/10.1016/j.compstruct.2020.112718

Huang, H., Wang, L., & Fan, Y. (2023). Metallic meta-biomaterials: A critical review of fatigue behaviours. *Journal of Science Advanced Materials and Devices, 8*(3). doi:https://doi.org/10.1016/j.jsamd.2023.100585

Kladovasilakis, N., Tsongas, K., & Tzetzis, D. (2020). Finite Element Analysis of Orthopedic Hip Implant with Functionally Graded Bioinspired Lattice Structures. *Biomimetics, 5*(3). doi:https://doi.org/doi.org/10.3390/biomimetics5030044

Libonati, F., Graziosi, S., Ballo, F., Mognato, M., & Sala, G. (2023). 3D-Printed Architected Materials Inspired by Cubic Bravais Lattices. *ACS Biomaterials Science and Engineering, 9*(7), 3935-3944. doi:https://doi.org/10.1021/acsbiomaterials.0c01708

Nazir, A., Abate, K., Kumar, A., & Jeng, J. (2019). A state-of-the-art review on types, design, optimization, and additive manufacturing of cellular structures. *International Journal of Advanced Manufacturing Technology, 104*, 3489-3510. doi:https://doi.org/10.1007/s00170-019-04085-3

Nguyen, D. (2019). Design of lattice structure for additive manufacturing in CAD environment. *Journal of Advanced Mechanical Design, Systems, and Manufacturing, 13*(3). doi:https://doi.org/10.1299/jamdsm.2019jamdsm0057

Plocher, J., & Panesar, A. (2019). Review on design and structural optimization in additive manufacturing: Towards next-generation lightweight structures. *Materials and Design, 183*. doi:https://doi.org/10.1016/j.matdes.2019.108164

Seharing, A., Azman, A., & Abdullah, S. (2020). A review on integration of lightweight gradient lattice structures in additive manufacturing parts. *Advances in Mechanical Engineering, 12*(6), 1-21. doi:https://doi.org/10.1177/1687814020916951

Szabó, K. (2022). Investigation of the Applicability of Topological Methods. In K. Jármai, & Á. Cservenák (Ed.), *Springer. Lecture Notes in Mechanical Engineering*, pp. 582-591. Vehicle and Automotive Engineering 4. doi:https://doi.org/10.1007/978-3-031-15211-5_49

Tao, W., & Leu, M. (2016). Design of lattice structure for additive manufacturing. *International Symposium on Flexible Automation*, (pp. 325-332). Cleveland, USA. doi:https://doi.org/10.1109/ISFA.2016.7790182

Voicu, A.-D., Hadăr, A., & Vlăs, D. (2021). Benefits of 3D printing technologies for aerospace. *Scientific Bulletin of Naval Academy, 29*, 8-16. doi:https://doi.org/10.21279/1454-864X-21-I1-001

Yang, Y., Song, X., Li, X., Chen, Z., Zhou, C., Zhou, Q., & Chen, Y. (2018). Recent Progress in Biomimetic Additive Manufacturing Technology: From Materials to Functional Structures. *Advanced Materials, 30*(36). doi:https://doi.org/10.1002/adma.201706539

Design of Machines and Structures, Vol. 14, No. 1 (2024), pp. 13–31.
https://doi.org/10.32972/dms.2024.002

CHRONICLES OF THE SEA: FROM ANCIENT GREEK GALLEYS TO MODERN MARVELS, JOURNEY TROUGH NAVAL HISTORY

RUBINA COLOMBO[1] – FERENC SARKA[2]

[1]*University of Genova, Via Opera Pia 15, 16145 Genova, Italy*
[2]*University of Miskolc, Institute of Machine and Product Design*
H-3515, Miskolc-Egyetemváros
[1]*rubinacolomboo@gmail.com*, [2]*ferenc.sarka@uni-miskolc.hu*
[2]*https://orcid.org/0000-0003-3136-4248*

Abstract: This publication attempts to present the history of the sailing ships development, from ancient times to the present day. It is almost impossible to present the development history of such an important technological achievement in a few pages, so we only focus on the most significant turning points in the publication. We present the ancient ships, the long ships of the Vikings, the shipbuilding techniques of the age of great geographical discoveries. We analyse the characteristics of line of ships, which greatly influenced the battles of the great powers of the world. Finally, we give a small overview of currently used sailing ship technologies.

Keywords: *naval history, ancient ship, sailing ship, line of ship*

1. INTRODUCTION

The history of sailing ships is a captivating journey spanning millennium, intricately woven into the fabric of human civilization. Over time, shipbuilding has been one of the driving forces behind the development of technology, which has been replaced by aviation in recent times. Humanity has always wanted to know and discover the unknown. From the beginning of mankind, we felt the urge to conquer the waters and the air. This article provides a concise exploration of the pivotal milestones in the evolution of sailing ships, tracing their development from prehistoric times to the present day. We present the typical ship types of the ancient times (Egypt, Rome). We mention the long ships created by the Vikings and their ship building technology. Famous ships of the age of great geographical discoveries (Nina, Pinta, Santa-Maria). Horatio Nelson's flagship, the HMS Victory, and then we will come to today's sailing ships developed with modern technology, to which the technical knowledge acquired in the science of aviation has already imparted to humanity and can predict the future vision of shipping.

2. Anatomy of a Sailing Ship

A sailing ship is a complex ensemble of carefully designed components that collectively ensure its functionality and navigation. From the commanding bow to the stern, the rear counterpart of ship, and the sides known as port and starboard, each part plays a crucial role. The right and left sides of the ships have been given separate names so that it is always clear regardless of the current position of the crew. The deck serves as the main horizontal surface, while the hull, submerged beneath the waterline, provides buoyancy, and houses essential compartments. Above the deck lies the superstructure, housing cabins and the command centre – the bridge. The mast rises vertically, supporting sails or navigation equipment, while the rudder at the stern controls the moving direction of the ship by manipulating the flow of water. In Figure 1 can be seen the parts of a regular sailing ship (Compton, 2014).

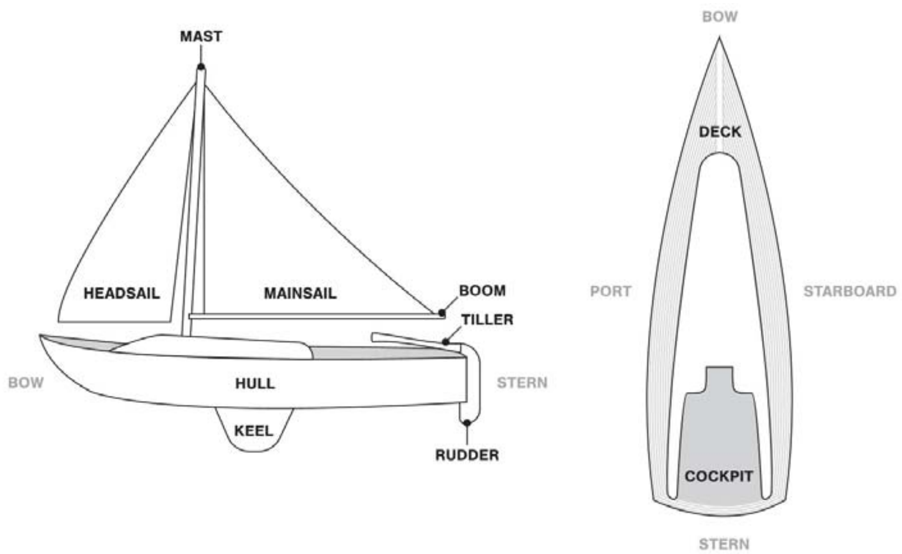

Figure 1. *The anatomy of sailing ship seen from the port (the left side of the vehicle) and from above*
https://www.sailrite.com/anatomy-of-a-sailboat

3. IMPORTANT STAGES IN SAILING SHIP HISTORY

The evolution of sailing ship has been profoundly influenced by technological advancements, economic demands, and strategic considerations. Several key stages mark this dynamic journey:

- ***Trade and Exploration:*** The expansion of maritime trade routes prompted the need for more efficient and capacious sailing ships. Innovations in hull design and rigging emerged to meet the growing demands of commerce.
- ***Navigation Technology:*** The development of navigation tools, from the compass to the sextant and the spring propelled mechanical clocks (John Harrison's (1693-1776) marine chronometer, the H4 from 1759), empowered sailors to navigate accurately across vast distances. These technological leaps influenced ship design to conquer diverse sea conditions.
- ***Military Needs:*** Naval powers drove innovations in shipbuilding to gain advantages in warfare. This led to the creation of various warships, emphasizing speed and manoeuvrability, shaping the evolution of sailboats.
- ***Scientific Inquiry:*** During the Age of Enlightenment, sailing ships became indispensable for scientific voyages. Expeditions led by figures like Captain James Cook (1728-1779) contributed to advancements in cartography, biology, and astronomy.
- ***Materials and Construction Techniques:*** The transition from wood to iron and eventually steel, along with improved construction methods, enhanced the durability and seaworthiness of sailboats, enabling larger and more complex designs.
- ***Cultural Exchange:*** Interaction between maritime cultures facilitated the exchange of shipbuilding knowledge. Techniques and designs from one region enriched the practices of another, fostering a global progression in sailing ship development.
- ***Competition and Innovation:*** Rivalry among maritime powers fuelled a competitive environment that propelled innovation. Each sought superiority in ship speed, cargo capacity, and naval dominance, resulting in continuous improvements in sailboat design.

In essence, the evolution of sailboats unfolds as a dynamic interplay of technological progress, economic imperatives, strategic considerations, and cultural exchange. This ongoing process has given rise to a diverse array of sailboat types, each optimized for specific purposes and conditions, contributing to the rich tapestry of maritime history (Anderson & Anderson, 2012).

4. Sailing Through Time: The Dynamic Evolution From Prehistory to Today

4. 1. Prehistory

Sailing, a practice rooted in ancient history, finds its origins in the humble beginnings of simple rafts and dugout canoes equipped with rudimentary sails crafted from animal hides or woven reeds (Figure 2).

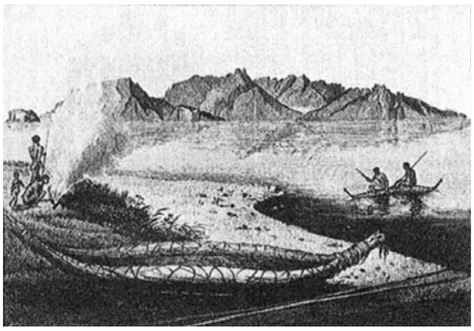

Figure 2. *The first boats: simple rafts or bark-bundle crafts (Johnstone, 1980)*

Early sailing vessels, initially used for fishing, transportation, and exploration, became crucial assets for civilizations like the Egyptians and Phoenicians. The maritime evolution of sailing witnessed notable contributions from the Egyptians and Phoenicians, particularly in the Atlantic tradition. Despite navigating both the Mediterranean Sea and the Atlantic Ocean, their influence diverged from other maritime cultures (Lavery, 2010). The earliest depiction of an Egyptian boat under sail dates back to 3500 BC, revealing reed rafts with masts on the Nile – a river pivotal to ancient Egyptian civilization. The discovery of the Cheops ship, a well-preserved artifact from 2600 BC, provides insight into ancient shipbuilding techniques. Although primarily a funeral ship, the Cheops (2589 BC-2566 BC) ship showcased the Egyptians' advanced maritime knowledge (Figure 3) (Leary, 2014).

By 2500 BC, wooden ships resembling river rafts emerged, facilitating trade along the Nile and the eastern Mediterranean coast. These flat-bottomed, square-ended vessels lacked a keel, limiting their size and suitability for coastal travel rather than open ocean navigation. While seagoing Egyptian boats resembled reinforced versions of river and coastal vessels, the Phoenicians, hailing from modern Lebanon, emerged as maritime experts in European antiquity. Despite limited evidence, Phoenician trading vessels with sturdy hulls and wooden plank decks revealed their prowess. By 1000 BC, Phoenician mariners ventured to Cornwall (Southwest part of the British Isle) for tin, and by 460 BC, they sailed as far as the Cape Verde Islands, marking a remarkable 2000-mile journey into the Atlantic Ocean. The work of the Phoenicians not confined only to trade, but they developed war galleys in response to Greek maritime competition, showcasing their versatility as seafarers. The Phoenician legacy in sailing underscores their crucial role in shaping ancient maritime history, setting the stage for further exploration and competition with emerging Mediterranean powers, particularly the Greeks (Lavery, 2010).

Figure 3. *Cheops ship (preserved in the Giza Solar boat museum, but was move to the Gran Egyptian Museum in August 2021) (Stein, 2017)*

4. 2. Ancient Civilizations

In the vast expanse of ancient maritime endeavours, the Greeks and Romans emerge as masterful architects, refining sailing technology and leaving an enduring legacy on naval warfare and trade in the Mediterranean.

Sailing Dynamics: A Balancing Act

Ancient boat speed, whether determined by oars or canvas, set the stage for the Greeks and Romans. While both civilizations engaged in maritime commerce using sailing vessels, their approach to naval warfare took a different course. The Greeks and Romans navigated the seas with oar-powered galleys, setting them apart from the slower, yet sturdy, trading ships of the time. The iconic slender galleys, revered as maritime icons in European antiquity, outshone their bulkier trading counterparts. This preference was a testament to the limitations of sailing know-how during this era, with rigging consisting of one or two masts carrying a single square sail.

Galleys: Masters of Naval Warfare

Galleys emerged as dominant forces in ancient naval warfare. The intricate dance of sails, wind, and oars required ample deck space, posing a challenge for warships that needed a clear area for soldiers. Consequently, oars became the preferred choice for warships due to their efficient use of deck space, a practical solution to the constraints posed by sails during battle (Figure 4). Before the advent of gunpowder and cannons, naval warfare was essentially a land battle at sea. Greek and Roman galleys engaged in ramming tactics, and if this failed, soldiers poured over the gunwales for hand-to-hand combat. The need for speed dictated the design, leading to longer galleys and the introduction of biremes and triremes, with some boasting up to 170 oarsmen, dominating Mediterranean waters from the 6th to the 4th century BC (Lavery, 2010).

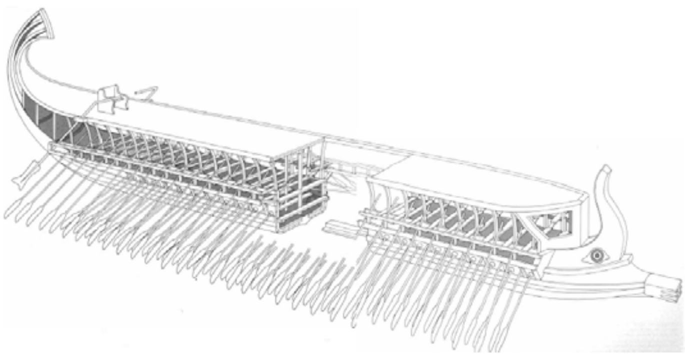

Figure 4. *An 18th-century engraving of a Roman warship © Stapleton Collection/CORBIS (Foley & Soedel, 1981)*

Roman Naval Supremacy: Quadriremes and Quinqueremes

As Rome succeeded Greece as the Mediterranean powerhouse, Roman galleys evolved into larger quadriremes and quinqueremes. The nomenclature here refers not to banks of oars but to the number of oarsmen per oar. Roman engineering prowess, coupled with influences from the Greeks and Carthaginians, propelled these galleys to dominance, lasting until the 5th century AD. These robust vessels served as troop transporters and formidable weapons platforms, capable of carrying 120 soldiers along with oarsmen. Disembarkation occurred via hinged gangplanks, resembling manoeuvres executed by World War II landing craft.

Merchant Ships: The Backbone of Trade

In contrast to the formidable war galleys, merchant ships played a crucial role in facilitating trade. The Mediterranean's relative safety from piracy allowed Roman merchants to flourish. Roman merchant vessels (Figure 5) adopted the proven design of Greek hulls, featuring symmetrical twin steering oars for effective manoeuvring. Despite challenges such as ship-worm damage and the absence of dry-dock facilities, Roman merchant ships thrived. Rigging improvements, including square-rigged sails and lateen rigs, contributed to their success. By the 5th century AD, Roman merchant ships dominated trade routes, notably importing vast quantities of grain from Egypt (Lavery, 2010).

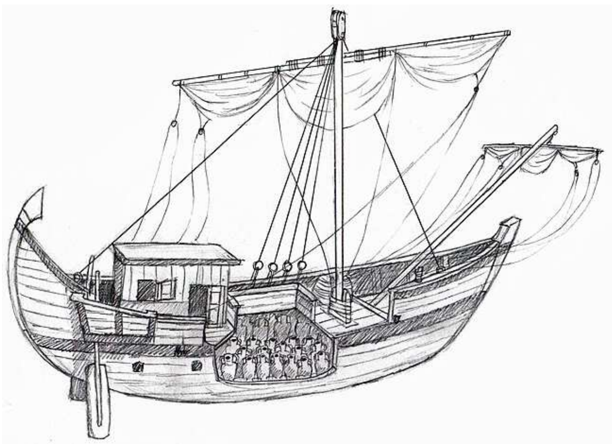

Figure 5. *Roman merchant ship*
(drawing made by Matthew Jose Fischer)

Legacy Unveiled: A Sailing Saga

In summary, the Greeks and Romans etched their indelible mark on ancient maritime history, refining sailing vessels for both war and trade. The legacy of their galleys and merchant ships paved the way for future advancements in naval architecture and navigation, leaving behind a sailing saga that resonates through the annals of time.

4. 3. Medieval and Renaissance Era

The Middle Ages saw the emergence of lateen sails, which greatly improved manoeuvrability and allowed sailors to sail closer to the wind. The Age of Exploration in the 15th and 16th centuries saw the development of caravels and other sailing ships that enabled long-distance ocean exploration by European powers like Portugal and Spain. Delve deeper into Columbus and la Nina (which is the sailing vessel).

Crafting the Seas: Clinker vs. Carvel Boat Building

Carvel construction (Figure 7), rooted in the eastern Mediterranean and influenced by ancient Egyptian barge building, ushered in a technique laying long planks for a sleek exterior. The strength of carvel boats emanates from the frame, enabling the creation of larger vessels despite the demand for meticulous labour. Carvel built wooden boats and tall ships are made by fixing planks to a frame with all the planks butting up against one another. This creates a smooth hull that's stronger than a clinker-built hull. However, more caulking is needed between the joints in carvel construction than in the clinker method. The framing gives carvel construction a stronger hull, allowing it to carry a full sail plan and have a longer, broader hull.
In the untamed landscapes of northern Europe, clinker construction (Figure 6) emerged, fuelled by the absence of precise saws. Using adzes, shipbuilders shaped the keel, stem, and stern posts, fashioning a robust outer shell with overlapping planks (Romey, 2017). Clinker built (or lapstrake) vessels are lighter as they have less internal framing –with the planks overlapping along their edges. As they're lighter, they displace less water allowing them to move faster. Clinker vessels are less rigid than carvel constructions, limiting the type of sailing rigs the vessel can take. In summary, this exploration of clinker and carvel construction transcends mere techniques, weaving a rich tapestry of maritime innovation, regional influences, and pragmatic adaptations. As the annals of boat-building history unfold, the legacy of clinker and carvel methods endures, leaving an indelible mark on naval architecture (Lavery, 2010).

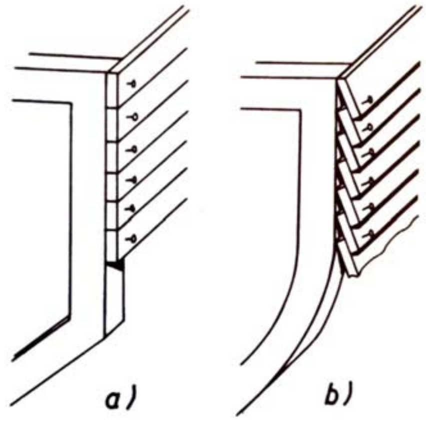

Figure 6. *Carvel (a) and Clinker (b) construction (Somoskői, 1984)*

Viking Longships: Marvels of Clinker-Built Mastery

The Viking longship represents the absolute maximum size for a clinker-built ships and vessels (Figure 7). These double-ended boats, boasting a T-shaped keel and low freeboard, were propelled by oars, particularly in their early days. Similar to Greek and Roman counterparts, Vikings utilized oars for warships and sails for merchant knarrs, such as the high-sided knarr. By 800 AD, the longship evolved, featuring a sizable square sail on a removable mast for sea voyages. Despite their open design and lack of a deck, these vessels undertook daring journeys, reaching as far as Iceland, Greenland, and Newfoundland by 1000 AD. The shallow draft of longships, influenced by their northern origins, made river exploration feasible, extending deep into Russia and the Black Sea. Unlike Mediterranean traditions, northern boatbuilders had not embraced symmetrically placed steering oars. Steering a longship was less intuitive than Roman galleys, with a single oar conventionally placed on the right side, leading to the term "starboard." Quay approaches required strategic manoeuvring, keeping the steering oar away to avoid damage. Regarded by many as the most beautiful boats of the first millennium AD, Viking longboats like the Oseberg and Gokstad ships have left an indelible mark. Archaeological treasures, such as the Oseberg ship from a ninth-century burial mound and the Gokstad ship from a tenth-century site in Norway, showcase their excellence. Replicas of these vessels, demonstrating their seaworthiness, have even crossed the Atlantic, echoing the enduring legacy of Viking clinker-built mastery (Lavery, 2010).

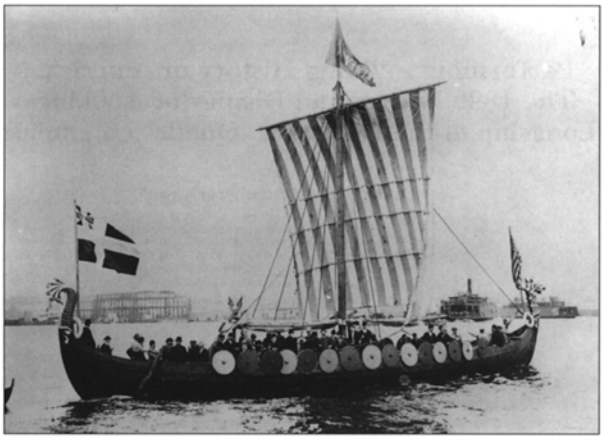

Figure 7. *A clinker-built Viking longship replica from 1893 (Andersson & Magelssen, 2017)*

The medieval contribution

The square sail (Figure 8 left) was the first and most common sail invented to aid rowers in propelling early ships and were dependent on wind direction. The Lateen sail (Figure 9 right) replaced the square rig beginning around the third century BC because it was more flexible and could adjust somewhat to the wind direction. In Europe, around 1200 BC, the square sail was in use on the large ships then being built and remained in use through the Age of Sail (from the mid-16th to the mid-19th centuries), adding a triangular lateen sail in the late 1400s for additional manoeuvrability (Campbell, 1995).

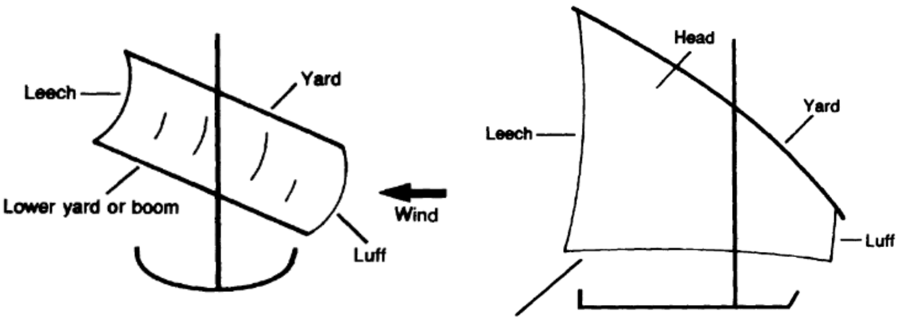

Figure 8. *The square sail (left), the Lateen sail (right) (Campbell, 1995)*

Sailing into the medieval era, the dissolution of the Roman Empire spurred a wave of innovation in shipbuilding. With fluid borders and evolving trade routes, the once-predictable voyages of merchantmen demanded vessels capable of navigating diverse wind and sea conditions, fostering the transition from oar-powered galleys to square-rigged sailing ships. Around the year 1000 AD, sailing technology witnessed a significant leap with the introduction of the lateen sail.

This triangular sail, suspended from a long, oblique yard, was influenced by Arab dhows, and found its place in Byzantine dromos. Dromos were that kind of warships that combined oar propulsion with substantial canvas sails. These vessels, showcasing both speed and manoeuvrability, marked a shift from traditional naval tactics, emphasizing long-range combat over ramming and boarding. In the eastern Mediterranean, the reign of dromos extended from the sixth to the twelfth century AD, sidelining the old square sail. Meanwhile, the clinker zone in northern and western Europe clung to the square sail due to rougher seas. The lateen sail excelled in the sheltered Mediterranean but struggled in the stormy North Sea and Atlantic. Notably, it allowed tacking into the wind, a capability absent in square sails limited to downwind or crosswind manoeuvres. A subsequent breakthrough emerged in the 12th century AD, as stern rudders made their debut in the cold waters of Scandinavia. It originates from China centuries earlier, this efficient steering mechanism spread through northern Europe, challenging the dominance of steering oars. While Mediterranean shipbuilders lagged in adopting stern rudders, the potential of this innovation extended beyond improved steering – it removed size constraints on ships, particularly in open ocean conditions. The explosive growth in sailing ship size arose from the marriage of clinker and carvel strands of the Atlantic tradition. As these two approaches converged, previously separate realms discovered the advantages held by the other, propelling a rapid evolution in sailing technology (Lavery, 2010).

The age of exploration Carrack and Caravel

Navigating the early fifteenth century, the Atlantic shipbuilding tradition experienced a surge, marking an era of remarkable sailing ship development. The blending of northern clinker and Mediterranean carvel designs, initiated during the Crusades, blossomed into a melting pot of ship-building ideas, culminating in the creation of the iconic carrack. The carrack, a carvel-built ship featuring a stern rudder, emerged as a groundbreaking vessel. Originating around Genoa in the fourteenth century, its evolution led to substantial size growth from 600 to 1,600 tons by the sixteenth century. Characterized by high sides, and castles on the stern, the carrack became a staple in Atlantic trade and exploration. Equipped with two to four masts and a fusion of square and lateen rigging, the carrack exemplified the convergence of northern and Mediterranean sailing technologies. Playing a pivotal role in the Age of Exploration, carracks like the Santa Maria accompanied Christopher Columbus to the New World in 1492, showcasing their seaworthiness (Figure 9). As the need for expanding trade and providing effective gun platforms converged, the carrack stood as a testament to the amalgamation of ship-building wisdom.

Figure 9. *Two caravels: Niña and Pinta and one carrack: Santa Maria (Romey, 2017)*

Alongside the carrack, the caravel emerged as a smaller but agile counterpart, originating in Portugal and associated with Iberian explorers. Typically measuring 20-25 m, the caravel boasted superior sailing characteristics, proving more manoeuvrable and faster than its larger counterpart. With variations in rigging, such as lateen or square sails, caravels excelled in windward sailing and remained the vessel of choice for open ocean exploration and trade until the late sixteenth century. In this dynamic period, the carrack and caravel symbolize the evolving maritime landscape, embodying the fusion of diverse ideas that shaped the course of naval history (Lavery, 2010). Sailing into the annals of maritime history, the Nina, a caravel of the fifteenth century, became an instrumental vessel in the Age of Exploration. Commissioned by Christopher Columbus for his legendary transatlantic voyages, the Nina exemplifies the pinnacle of caravel design. Measuring approximately 20 to 25 meters, the Nina was a nimble and seaworthy craft. Caravels like the Nina were carvel-built, featuring a shallower draft, a raised stern, and no forecastle. The hull design provided buoyancy and resistance to leeway, enhancing the ship's manoeuvrability and speed. The Nina was equipped with a distinctive aft castle built on the square stern, and with a practical deck. The rigging of the Nina, crucial to its exceptional sailing capabilities, typically included three or four masts, predominantly lateen-rigged. This sail arrangement allowed the caravel to harness the wind efficiently, making it adept at sailing into the wind, an invaluable trait for exploration voyages where varied wind conditions were encountered. Commissioned by Columbus for his historic journey to the New World in 1492, the Nina played a pivotal role in the first transatlantic crossing. Alongside its counterparts, the Pinta and the Santa Maria, the Nina ventured into uncharted waters, contributing significantly to the European exploration of the Americas. The agility of caravel and manoeuvrability made it suitable for navigating tight bays and close to rocky shorelines, essential qualities for exploration endeavours. As part of Columbus's fleet, the Nina carried the explorers across the Atlantic, showcasing the resilience and adaptability of caravels in the face of the unknown. The historic voyage, while fraught with challenges, marked a transformative moment in world history, with the Nina standing as a testament to the technological prowess and navigational expertise of its time. In the wake of Columbus's journey, the Nina remains an enduring symbol of exploration, embodying the spirit of adventure that defined the Age of Discovery (Lavery, 2010).

4. 4. 17th to 19th Century

The 17th century brought innovations like the frigate and brigantine (Figure 10), which were used by navies for both exploration and warfare. The frigates became renowned for their balanced combination of speed, firepower, and endurance. These ships were adaptable, serving various roles such as convoy protection, reconnaissance, and engaging enemy vessels. Brigantines, with their two-masted design, offered agility and versatility, making them valuable assets for both naval and private enterprises (Lavery, 2010).

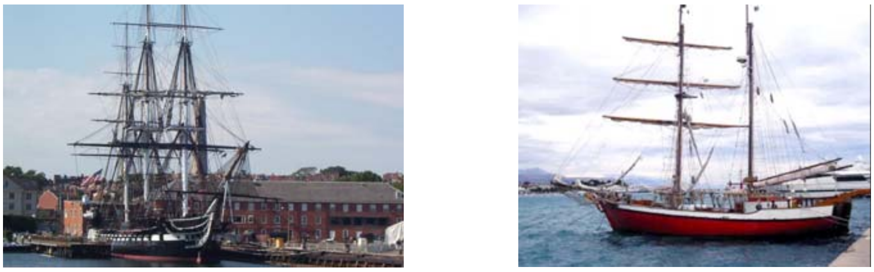

Figure 10. *Frigate sailing ship (left), Brigantine sailing ship (right) (Britannica Encyclopedia, 1974)*

The 18th century marked the Golden Age of Piracy, with pirates like Blackbeard (Edward Teach) operated sleek schooners, frigates and sloops, prized for their ability to navigate shallow waters. These ships were well-suited for surprise attacks, allowing pirates to exploit their targets with speed and precision.
The 19th century saw the transition from wooden sailing ships to iron and eventually steel, leading to the development of powerful warships and merchant vessels, revolutionized naval architecture. Ironclads, featuring iron armour, emerged as formidable warships, transforming naval warfare (Figure 11). This technological evolution extended to merchant vessels, enhancing their durability and cargo capacity. The transition from sail to steam power further propelled maritime innovation, enabling ships to traverse longer distances with increased efficiency (Lavery, 2010).

Figure 11. *Sail to steam propulsion. The Great White Fleet painting by John Charles Roach, 1984, depicting U.S. Atlantic Fleet battleships steaming at sea during their 1907–1909 World cruise. Courtesy of the U.S. Navy Art Collection, Washington, D.C. U.S. Naval History and Heritage Command photograph. Catalogue #: 95513-KN.*
https://www.history.navy.mil/browse-by-topic/communities/surface/steam.html

Overall, these centuries witnessed a dynamic evolution in ship design and technology, shaping the strategies of exploration, trade, and conflict on the high seas. The HMS Victory (Figure 12), a renowned ship of the line, epitomized naval power during the 18th and 19th centuries. The HMS Victory was launched at Chatham in 1765. She was a 100-gun ship of the line with a length of 186 feet (57 m), a load capacity of 2,162 tons, and a crew of more than 800 men (Britannica Encyclopedia, 1974). As a first-rate ship, it boasted an impressive three-gun decks, carrying a formidable array of cannons. Typically crewed by hundreds of sailors and marines, ships of the line like the HMS Victory were instrumental in major naval engagements, serving as the backbone of fleets. These vessels were characterized by their massive size, robust construction, and imposing firepower.

Figure 12. *HMS Victory*
(Britannica Encyclopedia, 1974)

The term "ship of the line" referred to their role in forming a line of battle, a strategic formation employed in naval warfare during this era. The imposing broadside of cannons, combined with sturdy hulls, made them formidable adversaries and key assets in securing maritime dominance. The HMS Victory, most famously associated with Admiral Horatio Nelson (1758-1805) and the Battle of Trafalgar in 1805, remains a symbol of naval supremacy and the peak of ship-of-the-line design and effectiveness during the Age of Sail (Lavery, 2010), (Britannica Encyclopedia, 1974).

4. 5. 20th Century to Present

The early 20th century witnessed the decline of sail in favour of steam and internal combustion engines for propulsion. Sailing for recreation and sport became increasingly popular, leading to the development of various sailboat classes and regattas. Modern sailing vessels often incorporate advanced materials, like fiberglass and carbon fibre, as well as computer technology for navigation and sail control. Today, sailing boats serve a wide range of purposes, from leisure and sport to cargo transportation and even cutting-edge racing competitions like the America's Cup. The history of sailing boats reflects humanity's enduring connection to the sea and the ongoing technological advancements that have shaped the world of sailing (Stalmokaitė et al., 2023).

Rotor sail: driving with the wind for environmentally friendly and economical sailing

Wind-Assisted Sail Propulsion (WASP) provides an ecological and economical solution for the growing maritime transport sector, responsible for 90% of global shipments. Currently, traditional ships emit significant amounts of air pollutants, contributing to an estimated annual carbon dioxide emission of 812 million tons. Rotor ships, based on the innovative Wind Propulsion Technology (WPT), offer a sustainable approach. The rotor drive concept has roots dating back almost a century, thanks to the German engineer Anton Flettner. Although past economic crises slowed the development of this technology, recent interest has been revived, exemplified by the Alcyone, a research vessel built in 1985. Rotor transmission harnesses the Magnus effect, known in sports and now applied technologically. As the rotor rotates, it creates an air pressure difference, generating a lateral force propelling the ship forward. This propulsion method enables efficient navigation, with the lateral force countered by the ship's hull. The rotation of the rotor cylinder, driven by a low-power motor, allows easy manoeuvrability, enabling the ship to move even in crosswinds. Additionally, adjusting the rotor direction ensures optimal performance in various weather conditions without the need to reduce sail area in strong winds. This technology offers additional advantages, including ease of control from a sheltered pilot position. In summary, rotor propulsion emerges as a promising solution for more sustainable maritime navigation, effectively combining ecological and economic benefits. The increasing demand for rotor solutions is experiencing a resurgence in maritime navigation. Several companies are experimenting with rotor sails to harness the opportunities of wind propulsion, yielding increasingly promising results.

Figure 13. *A rotor sail wind powers Scandlines (Werner S., Nisbet J., Hörteborn A., & Nielsen R., 2021)*

A pioneer in this field is the E-Ship 1, a modern cruiser measuring 130 meters, built in 2008 and operational since 2010. Equipped with 4-meter Flettner rotors mechanically linked to the propellers, this hybrid ship from the German company Enercon has demonstrated an average fuel saving of 25% compared to a ship with Mitsubishi diesel engines. In 2020, Scandlines successfully installed a rotor (Figure 13) on a four-year-old ferry, named Copenhagen (Figure 13), achieving a 5% reduction in carbon dioxide emissions.
Larger rotors, measuring 40x40 meters, are now in use on the Maersk Pelican. Other innovative solutions include rotors that can be laterally moved on the deck, as seen in the case of the 2017-built TR Lady, optimizing port loading. The SV Connector, a 12,000-ton Norwegian Ro-Ro ship, represents a step forward as the first tiltable rotor ship. Equipped with Norsepower sails, an advanced version of Flettner rotors, this vessel provides further insight into the ongoing evolution of wind propulsion technologies in modern maritime practices (Nuttall & Kaitu'u, 2016).

The Oceanbird: a fusion of tradition and technology

The Oceanbird (Figure 14) is a visionary concept in the maritime world, representing a cutting-edge approach to sustainable shipping. This innovative vessel is designed to harness wind energy, reducing reliance on traditional fuel sources and minimizing environmental impact. With its towering wing sails, the Oceanbird is a striking symbol of green shipping technology, aiming to revolutionize the industry by combining efficiency and eco-friendliness. As the maritime sector seeks solutions for a more sustainable future, the Oceanbird emerges as a promising and forward-thinking answer to the challenges of modern shipping (Stalmokaitė, Larsson Segerlind, & Yliskylä-Peuralahti, 2023). Is it a majestic vessel renowned for its sleek design and formidable performance, effortlessly navigates the open seas. With a harmonious blend of cutting-edge technology and timeless craftsmanship, this maritime masterpiece embodies the spirit of adventure and the thrill of the open water. From its meticulously crafted hull to the state-of-the-art rigging, every element of the Ocean Bird is a testament to the artistry and engineering prowess that define this extraordinary sailing vessel. From stem to stern, this sailboat exemplifies the marriage of tradition and innovation, inviting seafarers to embark on adventures with style and performance at the forefront. The Oceanbird provides wings for a shipping revolution. (Stalmokaitė, Larsson Segerlind, & Yliskylä-Peuralahti, 2023)

Figure 14. *The Oceanbird*
(Stalmokaitė, Larsson Segerlind, & Yliskylä-Peuralahti, 2023)

5. Summary

Summarizing what we learned at the end of our trip, we can say that shipping and sailing ships have played a significant role in the history of mankind. They made new discoveries possible not only in the geographical sense, but contributed to the development of mathematics, physics, biology and medicine. We still deserve to admire these brilliant engineering creations and remember with respect those people who served on sailing ships of different eras.

References

Anderson, R., & Anderson, R. (2012). *A short History of The Sailing Ship.* Dover Publications.

Andersson, A., & Magelssen, S. (2017). Performing a Viking History of America: The 1893 Voyage and Display of a Viking Longship at the Columbus Quadricentennial. *Theatre Journal, 69*(2), 175-195. doi:https://doi.org/10.1353/tj.2017.0023

Britannica Encyclopedia (15th ed., Vol. 29). (1974). Encyclopaedia Britannica (UK) Ltd.

Campbell, I. (1995). The Lateen Sail in World History. *Journal of World History, 6*(1), 1-23. Retrieved from http://www.jstor.org/stable/20078617

Compton, N. (2014). *The Anatomy of Sail.* London: Bloomsbury Publishing Plc.

Foley, V., & Soedel, W. (1981). Ancient Oared Warships. *Scientific American, 244*(4), 148-163. doi:https://doi.org/10.1038/scientificamerican0481-148

Freire, J., Farinha, N., Fialho, A., & Correia, F. (2007). Contributo para o estudo da tecnologia naval romana, a partir da reconstrução gráfica de um navio tipo Corbita. *Conimbriga, 46*, 281-290. doi:https://doi.org/10.14195/1647-8657_46_12

Johnstone, P. (1980). *The Sea-craft of Prehistory.* Routledge & Kegan Paul Ltd.

Lavery, B. (2010). *Ship: 5000 Years of Maritime Adventure.* Dorling Kindersley.

Leary, J. (2014). *Past Mobilities - Archaeological Approaches to Movement and Mobility.* Routledge. doi:https://doi.org/10.4324/9781315599632

Nuttall, P., & Kaitu'u, J. (2016). The Magnus Effect and the Flettner Rotor: Potential Application for Future Oceanic Shipping. *The Journal of Pacific Studies, 36*(2), 162-183. doi:https://doi.org/10.33318/jpacs.2016.36(2)-9

Romey, K. (2017). *Why haven't found Columbus' ships?* Retrieved from National Geographic: https://www.nationalgeographic.com/history/article/columbus-nina-pinta-santa-maria-shipwreck-archaeology

Somoskői, E. (1984). *Élethű versenyhajó modellek építése.* Budapest: Műszaki Könyvkiadó.

Stalmokaitė, I., Larsson Segerlind, T., & Yliskylä-Peuralahti, J. (2023, 2). Revival of wind-powered shipping: Comparing the early-stage innovation process of an incumbent and a newcomer firm. *Business Strategy and the Environment, 32*(2), 958-975. doi:https://doi.org/10.1002/bse.3084

Stein, S. (2017). *The Sea in World History.* ABC-CLIO.

Werner S., Nisbet J., Hörteborn A., & Nielsen R. (2021). Speed trial verification for a wind assisted ship. *International Conference on Wind Propulsion*, 61-72. doi:https://doi.org/10.3940/rina.win.2021.09

Design of Machines and Structures, Vol. 14, No. 1 (2024), pp. 32–42.
https://doi.org/10.32972/dms.2024.003

CONSTRUCTION OF THE CONTACT ZONE OF A HELICAL CYLINDRICAL EXTERNAL GEAR PAIR WITH STRAIGHT TOP LAND MERIDIANS

ZSUZSA DRÁGÁR

University of Miskolc, Institute of Machine and Product Design
3515 Miskolc-Egyetemváros
zsuzsa.dragar@uni-miskolc.hu
https://orcid.org/0000-0003-2028-7718

Abstract: The study deals with the construction of the contact zone of helical cylindrical external gears. The shape and size of the contact zone determine the phenomena that occur even in the case of error-free tooth design, installation error exemption and load-induced error exemption Such a phenomenon is the vibration excitation resulting from the connection, which also affects the identification of the drive elements. It is possible to deviate from the regular rectangular shape of the contact zone by modifying the top land surfaces. The change can mean a combination of the change in the total length of the contacting generating lines and the change in the contact ratio. This study deals with the construction of the generalized contact zone.

Keywords: *contact zone, contacting generating line, top land meridian*

1. The relationship between tooth directions and the components of the contact zone

When designing a gear pair, the geometry of the gears, their position relative to each other, the direction of the teeth and their direction of rotation are fixed. With this knowledge, it is possible to decide where the point of meshing in and the point of leaving meshing of the contacting generating lines are located in the contact zone (Erney, 1983), (Litvin F. , 1972). Figure 1 shows the two basic cases that help determine the arrangement of the contact zone. The pinion (small wheel) is the drive wheel, on which the teeth can be left (L) or right (R) tooth direction. On the driven wheel (gear), in the case of an external connection, the tooth direction must be opposite to this. The red dashed line marked on the wheels indicates the position of the recommended top land meridian modification.

In the lower part of Figure 1, the contact zone belonging to the meshing gears can be seen in the yz coordinate system. The contact zone is located in the contacting plane, which is the common tangent plane rolling down from the base cylinders of the gears, the common tangent plane of the base cylinders.
The size of the contact zone is determined in the y direction by the common tooth width, and in the z direction by the distance that the addendum cylinders cut out of the contacting plane in the transverse plane(s) (point A in the case of the large wheel and point E in the case of the small wheel). These points mark the point of meshing in (A) and the point of leaving meshing (E) in the case of deceleration drive. (The figure does not show the apparently increased part of the contact zone.)
The origin of the yz coordinate system is located in half of the common tooth width and on the component containing the main point C of the meshing. The slanted lines passing through points A and E indicate the contacting generating lines (the contact line of the meshing tooth sides).

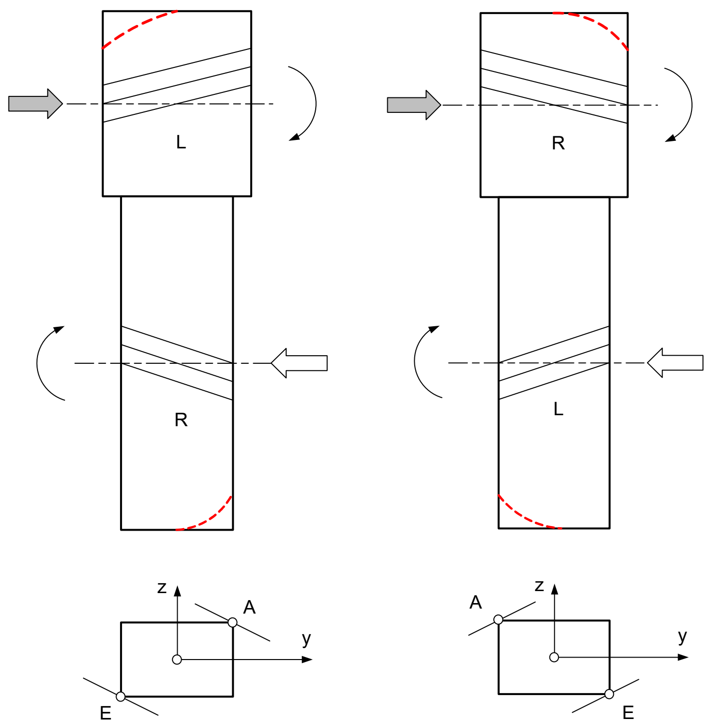

Figure 1. *Layout options for the contact zone*

2. KNOWLEDGE FROM GEAR PAIR DESIGN

There are many articles in the literature that talk about modifying the shape of the gear tooth. These usually deal with the modification of the profile (tip relief modification), crowning or end relief (Litvin, et al., 2003), (Litvin, Gonzalez-Perez, Fuentes, Hayasaka, & Yukishima, 2005), (Tran, Hsu, & Tsay, 2014), (Jamali, Sharif, Evans, & Snidle, 2015), (Yang, Wu, Li, & Liu, 2023). This article discusses the modification of the top land surface, as a result of which the shape of the contact zone changes.

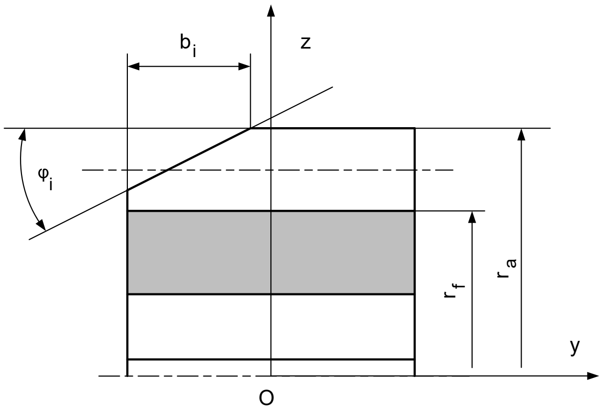

Figure 2. *Drawing representation of the top land meridian modification*

Based on the knowledge about the contact zone (Graf von Seherr-Thoss, 1965), (Debreczeni, 2021), the designer, deviating from the top land meridian that defines the regular rectangular contact zone, creates it with several well-defined lines compared to each other. Figure 2 shows a detail of a gear drawing, where a single line represents the modification, but there can be several of them. For further investigations, let's follow the drawing definition of a straight line. The gear should be defined in the „O” centred coordinate system with the parameters specified by the designer.

The top land of the tooth should be truncated by a straight line given by the parameters φ_i, b_i shown in Figure 2. To construct the contact zone, the design data must be transformed and the identification of the meridian consisting of several straight lines (Figure 3) must also be taken into account.

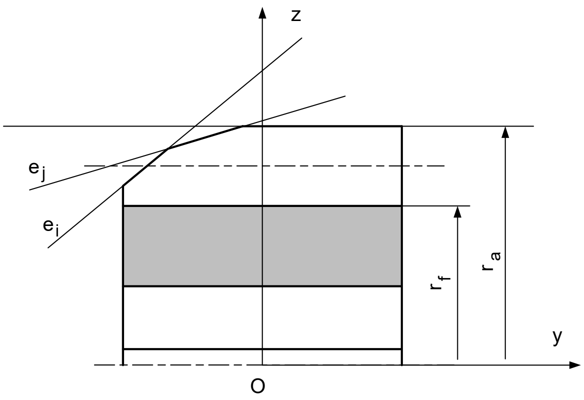

Figure 3. *Example of a meridian element consisting of several straight lines*

The i[th] line element of the meridian, which generates the top land surface and also maps the borders of the contact zone, is interpreted according to Figure 4. The meridian element also intersects the axis of the gear wheel, which should be marked by point $K_i(y_{Ki}, z_{Ki})$.

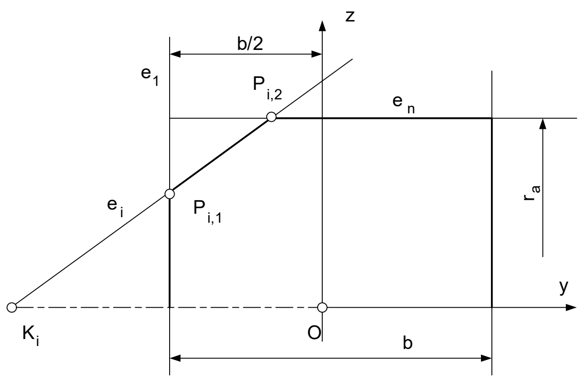

Figure 4. *Definition of a meridian straight line*

Let n be the number of straight lines that make up the axial section of the space enclosed by the transverse surface of the gear on the modification side and the addendum cylinder. Among the straight lines defining the transverse surface, the first $y = -\frac{b}{2}$ is parallel to the z axis. The last (n-th) straight line, usually parallel to the axis of rotation, is the generator of the addendum cylinder, whose equation is $z =$

r_a. The additional elements of the meridian have a number of $k = n - 2$, i.e. if the modification contains k elements, then the number of straight lines to be examined is $n = k + 2$. Points that define the i[th] line have coordinates $P_{i1}(y_{i1}, z_{i1})$and $P_{i2}(y_{i2}, z_{i2})$. (Figure 5).

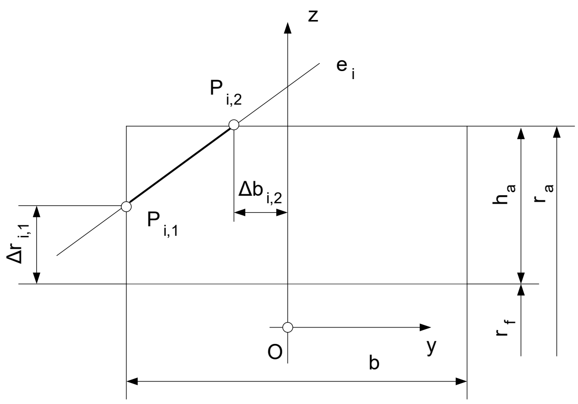

Figure 5. *Determining points of the meridian elements*

By definition, the possibility of changing the radial direction is possible in the range of height h_a designated by the dedendum and addendum cylinders:

$$h_a = r_a - r_f \tag{1}$$

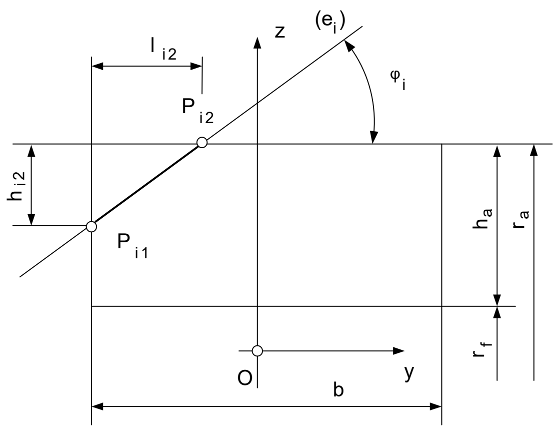

Figure 6. *Drawing geometry*

The coordinates of the two points of the i[th] line are $P_{i1}\left(-\frac{b}{2}, r_f + \Delta r_{i1}\right)$ and $P_{i2}(-\Delta b_{i2}, r_a)$. Values Δb_{i2} and Δr_{i1} can be obtained from the drawing documentation. In the drawing documentation, Figure 2 presented the design data for a meridian line of the wheel, which can be generalized to a straight meridian element of any position with the help of Figure 6.
With the dimensions given in the drawing

$$h_{i1} = l_{i2} \cdot \tan \varphi_i \tag{2}$$

from which

$$\Delta r_{i1} = h_a - h_{i1} \tag{3}$$

Forming a ratio factor a_i

$$a_i = \frac{\Delta r_{i1}}{h_a}, \quad (0 \le a_i \le 1) \tag{4}$$

which can be used to select any point if a_i is chosen freely. The value of Δb_{i2} can be determined from half the tooth width:

$$\Delta b_{i2} = \frac{b}{2} - l_{i2} \tag{5}$$

which can also be specified with a ratio factor:

$$c_i = -\frac{\Delta b_{i2}}{0{,}5b}, \quad (-1 \le c_i \le 1). \tag{6}$$

3. GENERALIZATION OF THE FORMATION OF MERIDIAN STRAIGHT LINES

As can be seen in Figure 4, the supporting points of the straight lines forming the meridian of the top land are located on the transverse surface of the gear wheel $P_{i1}(y_{i1}, z_{i1})$ and on the addendum cylinder $P_{i2}(y_{i2}, z_{i2})$. It has already been seen in the previous sections that these points can be read from the drawing documentation of the gears or can be specified based on subsequent design modifications. However, it is advisable to calculate these from the zone modification inferred based on practice. The equation of the i-th generalizable line can be given according to the following procedure.
The coordinates of a pair of points can be systematized in the matrix:

$$\boldsymbol{P}_{(n\times 4)} = \begin{pmatrix} y_{11} & z_{11} & y_{12} & z_{12} \\ y_{21} & z_{21} & y_{22} & z_{22} \\ \vdots & \vdots & \vdots & \vdots \\ y_{n1} & z_{n1} & y_{n2} & z_{n2} \end{pmatrix},$$

the elements of which are denoted by $p_{ij}(i = 1,2,\dots,n; j = 1,2,3,4)$. The equation of the i^th^ line can be expressed as follows with the elements of the matrix:

$$\begin{gathered} \frac{p_{i4} - p_{i2}}{p_{i3} - p_{i1}} \cdot (y_i - p_{i1}) = z_i - p_{i2} \\ z_i = \frac{p_{i4} - p_{i2}}{p_{i3} - p_{i1}} \cdot y_i + p_{i2} - \frac{p_{i4} - p_{i2}}{p_{i3} - p_{i1}} \cdot p_{i1} \end{gathered} \tag{7}$$

from which:

$$z_i = m_i \cdot y_i + b_i, \tag{8}$$

where:

$$m_i = \frac{p_{i4} - p_{i2}}{p_{i3} - p_{i1}}, \tag{9}$$

$$b_i = p_{i2} - \frac{p_{i4} - p_{i2}}{p_{i3} - p_{i1}} \cdot p_{i1}. \tag{10}$$

Within the interpretation range of y_i, the z_i coordinate can be calculated for any y_i coordinate, which is always the current addendum circle radius interpreted on the gear meridian.

4. THE INTERPRETATION RANGE OF THE TOP LAND MERIDIAN, DEFINITION OF INTERSECTION POINTS

The top land meridian consists of straight lines whose intersection points determine the interpretation range of each line along the width. Figure 7 illustrates the interpretation range along the tooth width for the ith line. By selecting the ith line of the meridian, then adding the $(i-1)^{th}$ line and the $(i+1)^{th}$ line, they create the M_i, M_{i+1} intersection points with their intersection points. On the ith straight line, the definition of the addendum circle radii is interpreted only in the range Δy_i where:

$$y_i \leq y \leq y_{i+1}. \tag{11}$$

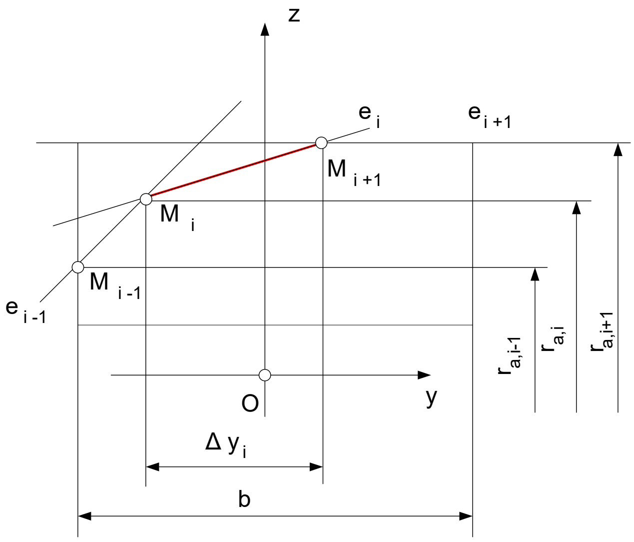

Figure 7. *Interpretation range of meridian elements*

The z coordinates determine the current addendum circle radii (r_a), i.e.
$r_i \leq r_a \leq r_{i+1}$.
The intersection point of two arbitrary lines (i and $i+1$) can be determined from the equations of the lines (7-10) if $z_i = z_{i+1}$, i.e.

$$m_i \cdot y_i + b_i = m_{i+1} \cdot y_i + b_{i+1} \tag{12}$$

from which

$$y_i = \frac{b_{i+1} - b_i}{m_i - m_{i+1}}, \tag{13}$$

and

$$z_i = r_{a,i} = m_i \cdot \frac{b_{i+1} - b_i}{m_i - m_{i+1}} + b_i. \tag{14}$$

To facilitate further analysis, let's introduce $M_i^1(y_i^1, z_i^1)$ to mark the intersection point belonging to the drive wheel, and $M_i^2(y_i^2, z_i^2)$ to mark the intersection point belonging to the driven wheel.

5. THE RELATIONSHIP BETWEEN THE INTERSECTION POINTS OF TOP LAND MERIDIANS AND THE CONTACT ZONE

The top land meridian is rotated around the axis of the gear wheel to create the top land surface (Roth, 1989a), (Roth, 1989b). The parts of the top land surface marked by intersection points are cone and cylinder surfaces. One boundary of the contact zone is determined by the intersection of these surface elements and the contacting plane (zone lower border), the other boundary is formed by the top land surface of the meshing gear with the contacting plane (zone upper border) (Figure 8). The driving wheel creates the zone lower border, the driven wheel creates the zone upper border. Contacting generating lines defining a meshing are interpreted only in the zone.

If the teeth of a gear wheel are not symmetrical, i.e. the base profile angles of the tooth sides are different, then depending on the direction of rotation, two different contact zones are formed (Drágár & Kamondi, 2018).

The intersection points determined on the top land meridian also form intersection points in the contact zone. Between the intersection points, which are formed as a section of a conic surface, a hyperbola section is the zone wrapper. In the future, it must be verified whether these sections can be replaced by straight lines, because then the meshing phenomena taking place in the contact zone can be examined more simply.

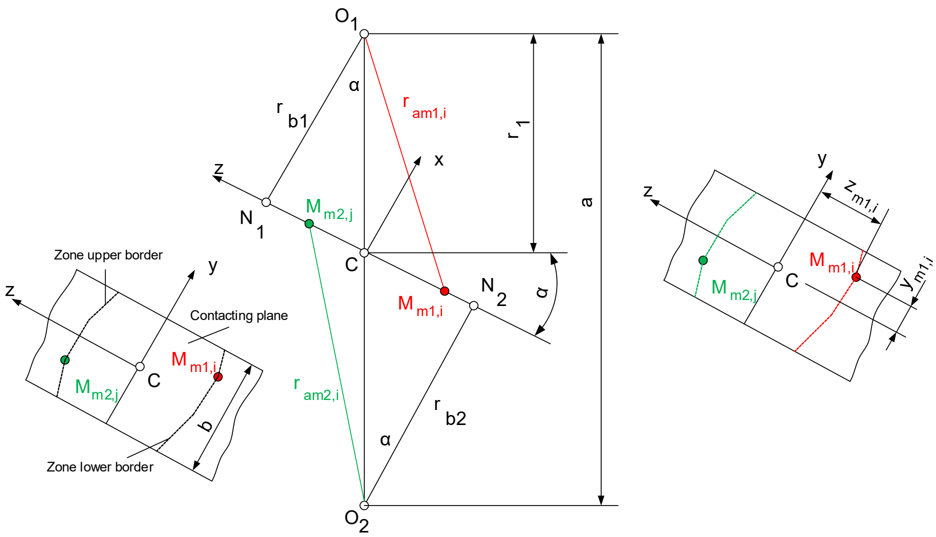

Figure 8. *Intersection point determined by the z coordinate of the contact zone*

The intersection point (M_i) determined on the meridian curve appears in the contact zone as the zone border point (M_{mi}) and its position can be calculated using the geometric data of the gear wheel (Drágár & Kamondi, 2021). Among the coordinates of the zone point, the y direction is identical to the similar coordinate of the point of intersection, z is to be determined, the generalized shape of which is

$$z_{mj,i} = \sqrt{\left(r_{amj,i}\right)^2 - \left(r_{bj}\right)^2} - \sqrt{\left(r_j\right)^2 - \left(r_{bj}\right)^2}, \tag{15}$$

when j = 1 drive wheel, j = 2 driven wheel, and i is the generalized intersection point.

6. Conclusions, results

The study presented the process in which the contact zone can be determined by knowing the geometry of the gears and the necessary tests can be performed in it. The meridian of the top land surface can be described in an easy-to-use and generalizable form with the presented description. The shape of the meridian elements (straight or higher order) between the intersection points (intersection planes) can also be chosen freely. The designer of the gear wheel has the freedom to shape the top land meridian according to his own vision, but at the same time, due to the role of the gear wheel in the drive, he may also require a special modification of the top land meridian. The presented procedure can help the designer to make quick and targeted modifications, as the method is also suitable for an automatic (expert) solution procedure, therefore, it gives the opportunity to be part of the planning assistance system in a computer program.

References

Debreczeni, D. (2021). Evolvens, külsőfogazatú, hengeres fogaskerékpárok fogtő teherbírásának és egyfogpár merevségének geometriai függősége.

Drágár, Z., & Kamondi, L. (2018). The role of the tooth shape in powertrains containing gears. *26th. International Conference on Mechanical Engineering, OGÉT 2018*, 232-235.

Drágár, Z., & Kamondi, L. (2021). The effect of the contact zone of cylindrical helical gears on the meshing and some considerations for determining its shape. *Design of Machines and Structures, 11*(1), 16-26. https://doi.org/10.32972/dms.2021.002

Erney, G. (1983). *Fogaskerekek.* Budapest: Műszaki Könyvkiadó.

Graf von Seherr-Thoss, H. (1965). *Die Entwicklung der Zahnrad-Technik.* Berlin: Springer-Verlag. https://doi.org/10.1007/978-3-642-92906-9

Jamali, H., Sharif, K., Evans, H., & Snidle, R. (2015). The Transient Effects of Profile Modification on Elastohydrodynamic Oil Films in Helical Gears. *Tribology Transactions, 58*(1), 119-130. https://doi.org/10.1080/10402004.2014.936990

Litvin, F. (1972). *A fogaskerékkapcsolás elmélete.* Budapest: Műszaki Könyvkiadó.

Litvin, F., Fuentes, A., Gonzalez-Perez, I., Carvenali, L., Kawasaki, K., & Handschuh, R. (2003). Modified involute helical gears: computerized design, simulation of meshing and stress analysis. *Computer Methods in Applied Mechanics and Engineering, 192*(33-34), 3619-3655. https://doi.org/10.1016/S0045-7825(03)00367-0

Litvin, F., Gonzalez-Perez, I., Fuentes, A., Hayasaka, K., & Yukishima, K. (2005). Topology of modified surfaces of involute helical gears with line contact developed for improvement of bearing contact, reduction of transmission errors, and stress analysis. *Mathematical and Computer Modelling, 42*(9-10), 1063-1078. https://doi.org/10.1016/j.mcm.2004.10.028

Niemann, G., & Winter, H. (1983). *Maschinenelemente.* Berlin, Heidelberg: Springer Berlin Heidelberg.

Roth, K. (1989a). *Zahnradtechnik. Band I. Stirnradverzahnungen-Profilverschiebungen, Toleranzen, Festigkeit.* Berlin: Springer Verlag.

Roth, K. (1989b). *Zahnradtechnik. Band II. Stirnradverzahnungen-Geometrische Grundlagen.* Berlin: Springer Verlag.

Tran, V.-T., Hsu, R.-H., & Tsay, C.-B. (2014). Tooth contact analysis of double-crowned involute helical pairs shaved by a crowning mechanism with parallel shaving cutters. *Mechanism and Machine Theory, 79*, 198-216. https://doi.org/10.1016/j.mechmachtheory.2014.04.012

Yang, Y., Wu, Y., Li, Y., & Liu, X. (2023). Effects of Tooth Modification in the Involute Helical Gear Form-Grinding Process on Loaded Transmission Character with Consideration of Tooth Axial Inclination Error. *Machines, 11*(2), 305. https://doi.org/10.3390/machines11020305

Design of Machines and Structures, Vol. 14, No. 1 (2024), pp. 43–51.
https://doi.org/10.32972/dms.2024.004

INVESTIGATION OF REMESHING PARAMETERS FOR DEVIATION ANALYSIS IN REVERSE ENGINEERING

PÉTER FICZERE

Budapest University of Technology and Economics,
Department of Railway Vehicles and Vehicle System Analysis,
1111, Budapest, Műegyetem rkp. 3
ficzere.peter@kjk.bme.hu
https://orcid.org/0000-0003-3207-5501

Abstract: The use of additive manufacturing technologies in industry is increasingly common, particularly with the emergence of Industry 4.0. These technologies can produce parts quickly and efficiently, but they also place higher demands on the quality of the manufactured products. The layer-by-layer processes create an anisotropic material model, which complicates component sizing. While the topic has been extensively researched, surface anisotropy has received less attention. The surface quality of a product may be affected by various factors, including the file conversion process or the staircase effect generated by the technology. Manufacturing parameters, such as layer thickness and orientation, can also have an impact. This paper focuses on the impact of reverse engineering step adjustment on surface quality.

Keywords: *reverse engineering, remesh, stl, deviation analysis, surface roughness*

1. INTRODUCTION

Today, additive manufacturing technologies are being used in more places and on an increasing scale. Additive manufacturing technologies are increasingly used in various applications due to their ability to meet the requirements of Industry 4.0 (Albert & Takács, 2023). However, the requirements for the components manufactured using this technology are also increasing. The layer-by-layer approach creates an anisotropic material model, making component sizing a more complex task (Kovács & Kovács, 2008). This topic has been researched extensively, but surface anisotropy has received less attention (Ahn, Kweon, Kwon, Song, & Lee, 2009), (Jin, Li, He, & Fu, 2015), (Pérez, 2002). This may be due to various reasons, such as the file conversion required for manufacturing preparation, as well as the staircase effect resulting from the technology used (2.5D machining) (Kónya & Ficzere, 2023), (Pandey, Venkata Reddy, & Dhande, 2003). Additionally, the surface quality of the final part is influenced by the manufacturing parameters such as layer thickness and orientation. There are various ways to enhance the surface quality (Kónya & Ficzere, 2024), (Hanon, Alshammas, & Zsidai, 2020), (Ficzere & László, 2023). However, discussions often revolve around the accuracy of manufacturing equipment, machines, and printers when inspecting, checking, and measuring a completed, manufactured part (Dömötör, 2023). It is important to note that these control measurements also have their own level of accuracy, which may result in errors in the system. It is possible that the measurement is inaccurate rather than the part itself (Makkai & Sarka, 2023). This paper illustrates the effect of adjusting a reverse engineering step used in a back-measurement.

2. METHODOLOGY

In 3D printing, layer-by-layer construction results in a staircase effect. The magnitude of this staircase effect depends on the position of the surface, so even if the printer is accurate, an error is made in the design of the toolpaths. A test part is shown in Figure 1, which illustrates the staircase effects caused by different shape features. The same shape accuracy results in different surface quality depending on the orientation.

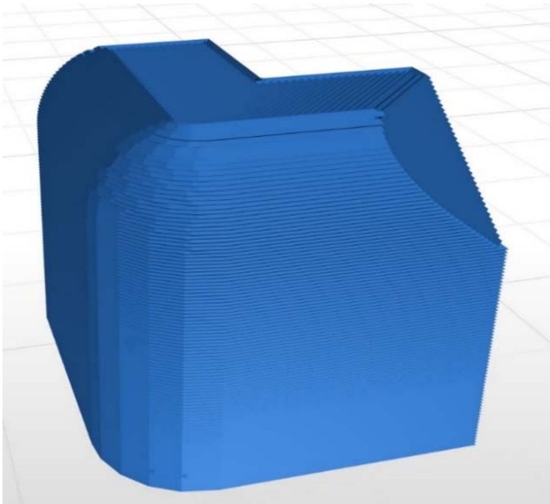

Figure 1. *Toolpath in slicer software*

Another unavoidable error is that we introduce varying degrees of error into the system when we select the layer height, a step that also affects printing speed. But even before these steps, errors are introduced during the conversion from CAD geometry to a standard triangular language (stl) file for the machine. Of course, with careful planning and thoughtful tolerances, the amount of error can be reduced to almost nothing during file conversion. The results of file conversion with different tolerances are shown in Figure 2. It is clear from the figure that when the file conversion tolerances are reduced, only the curved surfaces change in the resulting stl file. The finer the tolerance, the better it follows the original CAD geometry.

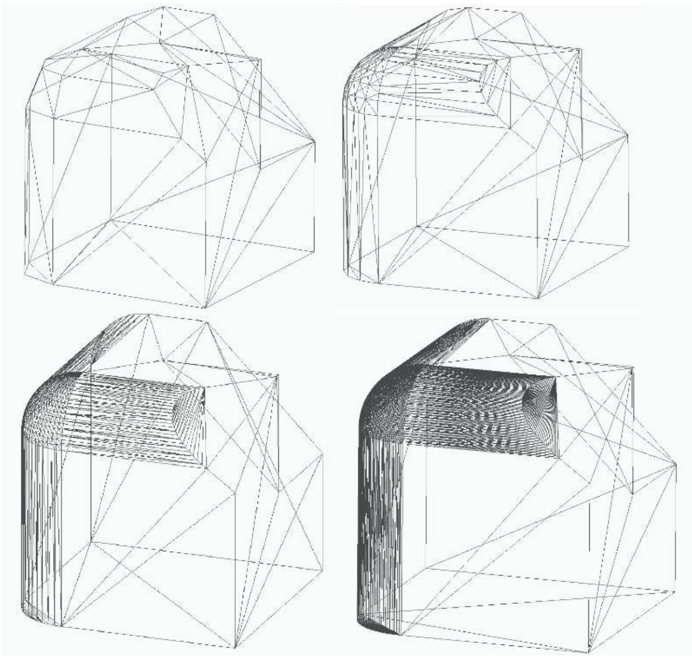

Figure 2. *CAD-stl file conversations with different tolerances*

In this study, the deviations of the part resulting from the coarsest stl conversion (top left in Figure 2) are investigated using reverse engineering methods. Today, most CAD software has a reverse engineering module. Here we have the possibility to perform deviation analysis. However, it should be noted that in the case of very coarse stl (as in the case under study), it is not possible to compare CAD and stl geometry in one step due to the large mesh sizes. We will also see later that even if it were possible, it is not practical because the coarse mesh distorts the results significantly. It is therefore advisable to remesh the stl geometry. In this case, the geometry under consideration is covered with smaller, uniformly distributed triangular elements. Such a remeshed geometry is shown in Figure 3.

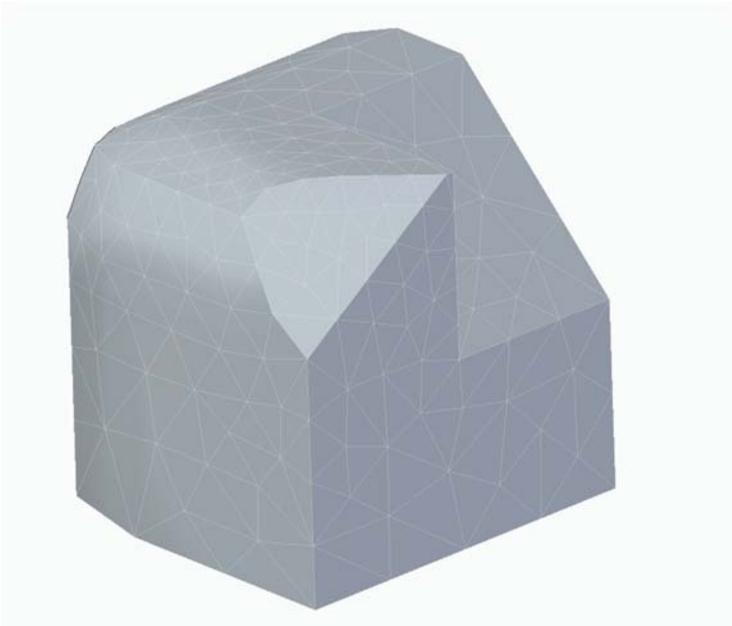

Figure 3. *Remeshed stl model*

The remeshed geometry shown in Figure 3 has been covered with triangular facets with an average element size of 6.75 mm. A comparison can now be made with the original CAD geometry. However, it is worth comparing the mesh shown in Figure 3 with the mesh shown in Figure 2, top left, where the difference is significant. We will now investigate how modifying the average element size used as a parameter for remeshing affects the accuracy of determining the deviation from the original CAD geometry.

3. RESULTS

The coarse stl mesh was remeshed with five different average element sizes (6.75 mm, 1 mm, 0.5 mm, 0.3 mm, 0.1 mm) to investigate the deviations from the original CAD geometry. Figure 4 shows the result of the deviation analysis after remeshing with the largest element size of 6.75 mm.

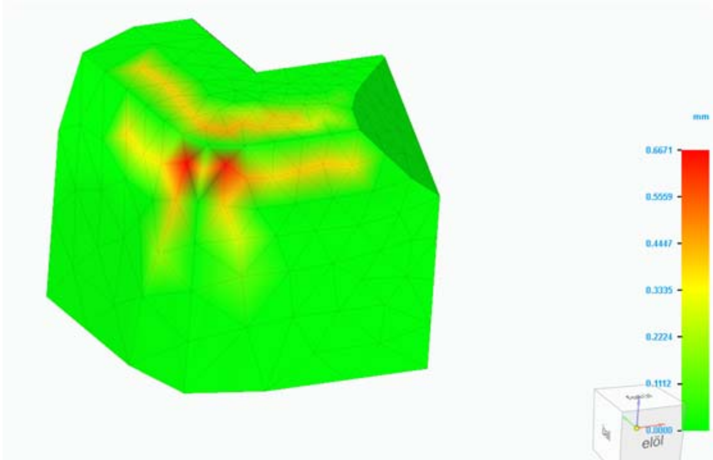

Figure 4. *Deviation analysis on remeshed (6.35 mm) coarse stl model*

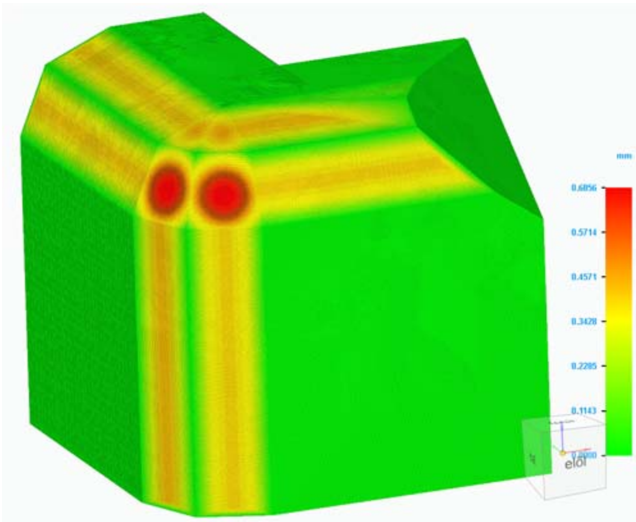

Figure 5. *Deviation analysis on remeshed (0.1 mm) coarse stl model*

It worth noting that this mesh density is not sufficient in critical areas with large deviations. Compared to the results of the analysis with an average element size of 0.1 mm shown in Figure 5, the difference is impressive and significant. The results obtained are shown in Table 1 as a function of the number of elements and the average element size.

Table 1

Deviations depending on element sizes

Element size (mm)	**Number of elements**	**Deviation (mm)**
6.75	236	0.667064
1	2594	0.678177
0.5	10449	0.679614
0.3	31482	0.685532
0.1	289128	0.685623

4. ANALYSIS

In Figure 6 we can visually observe the results of the deviation analysis for the different mesh densities.

A more detailed examination of the figure shows that even at low mesh densities the deviations from the CAD geometry are of a different nature. For example, in the upper left part of Figure 6 the deviations are only patchy, whereas in the lower right part of the figure (element size 0.3 mm) the bands along the roundings are clearly visible.

Irrespective of the numerical values, it can be seen, as expected, that there are no deviations from the CAD geometry on the flat surfaces, while there are deviations on the curved surfaces (roundings). It is also clear that the deviation varies along the curvature, which was also expected. These findings confirm that the deviation analysis within the reverse engineering module is fit for purpose, the results are in accordance with the theoretical background.

However, it is also interesting to note that the deviations are even more significant for double roundings (corner rounding, spherical surface).

It is useful to examine the numerical results in the shape of a diagram. In this way, the nature and shape of the curve can be used to determine whether an appropriate mesh density has been used. The results of the present study are presented in a diagram in Figure 7.

It can be seen that for small numbers of elements, although the shape of the curve changes significantly, the accuracy deviation is still less than 0.15 mm. Naturally, this depends on many things, so it is advisable to plot such a convergence curve for each individual part.

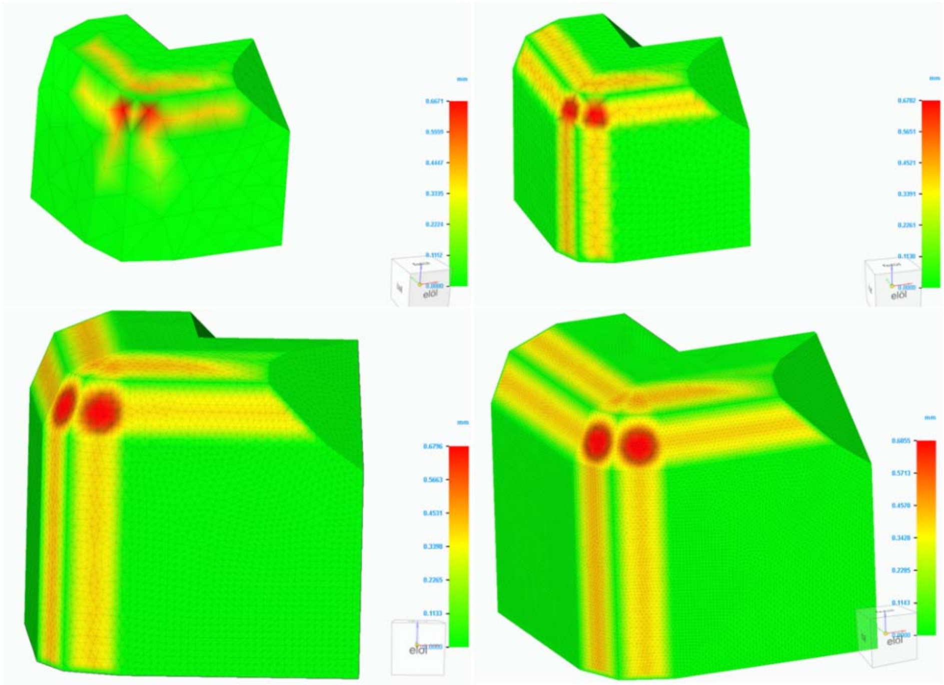

Figure 6. *Deviation analysis with different element sizes in remeshing*

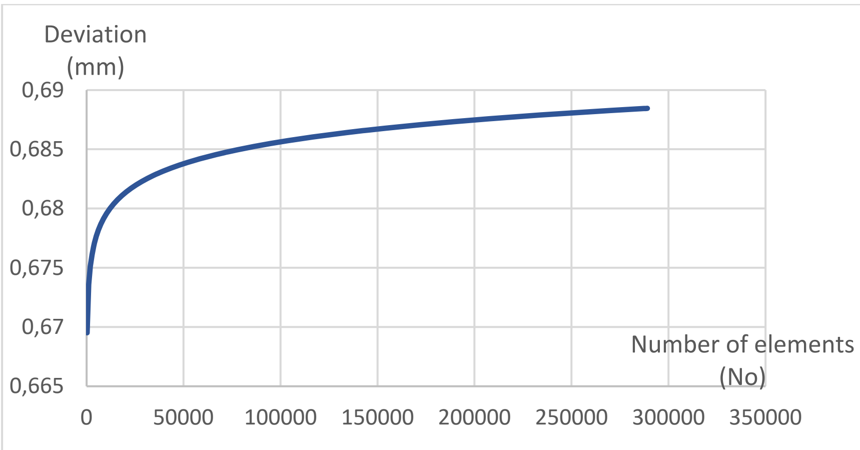

Figure 7. *Deviations as function of the number of surface elements*

5. SUMMARY

In summary, although our software is now capable of very high accuracy, without the right theoretical background we can make significant errors in file conversions, measurements and revalidation. It is therefore worth being cautious when judging the accuracy of production equipment.

REFERENCES

Ahn, D., Kweon, J.-H., Kwon, S., Song, J., & Lee, S. (2009, 8). Representation of surface roughness in fused deposition modeling. *Journal of Materials Processing Technology, 209*(15-16), 5593-5600. doi:https://doi.org/10.1016/j.jmatprotec.2009.05.016

Albert, J., & Takács, Á. (2023). Additív gyártás biomimetikai megközelítéssel. *GÉP, 74*(4), 9-12.

Dömötör, C. (2023). Reconstruction of Simple Parts Using FDM Technology. *Design of Machines and Structures, 13*(2), 13-21. doi:https://doi.org/10.32972/dms.2023.013

Ficzere, P., & László, N. (2023). Surface Modification Methods of Plastic Components Produced by Additive Manufacturing: A Review. *Design of Machines and Structures, 13*(2), 53-68. doi:https://doi.org/10.32972/dms.2023.017

Hanon, M., Alshammas, Y., & Zsidai, L. (2020, 5). Effect of print orientation and bronze existence on tribological and mechanical properties of 3D-printed bronze/PLA composite. *The International Journal of Advanced Manufacturing Technology, 108*(1-2), 553-570. doi:https://doi.org/10.1007/s00170-020-05391-x

Jin, Y.-a., Li, H., He, Y., & Fu, J.-z. (2015, 10). Quantitative analysis of surface profile in fused deposition modelling. *Additive Manufacturing, 8*, 142-148. doi:https://doi.org/10.1016/j.addma.2015.10.001

Kónya, G., & Ficzere, P. (2023). The Effect of Layer Thickness and Orientation of the Workpiece on the Micro- and Macrogeometric Properties and the Machining Time of the Part during 3D Printing. *Periodica Polytechnica Mechanical Engineering, 67*(2), 143-150. doi:https://doi.org/10.3311/PPme.21473

Kónya, G., & Ficzere, P. (2024). The Effect of Layer Thickness and Orientation of 3D Printed Workpieces, on The Micro- and Macrogeometric properties of Turned Parts. *Acta Polytechnica Hungarica, 21*(2), 231-250. doi:https://doi.org/10.12700/APH.21.2.2024.2.13

Kovács, N., & Kovács, J. (2008). Developments in the Field of Rapid Prototype Production. *Materials Science Forum, 589*, 421-425. doi:https://doi.org/10.4028/www.scientific.net/MSF.589.421

Makkai, T., & Sarka, F. (2023). CAD Modelling of a Milling Insert. *Design of Machines and Structures, 13*(2), 81-92. doi:https://doi.org/10.32972/dms.2023.019

Pandey, P., Venkata Reddy, N., & Dhande, S. (2003). Improvement of surface finish by staircase machining in fused deposition modeling. *Journal of Materials Processing Technology, 132*(1-3), 323-331. doi:https://doi.org/10.1016/S0924-0136(02)00953-6

Pérez, C. (2002). Analysis of the surface roughness and dimensional accuracy capability of fused deposition modelling processes. *International Journal of Production Research, 40*(12), 2865-2881. doi:https://doi.org/10.1080/00207540210146099

Design of Machines and Structures, Vol. 14, No. 1 (2024), pp. 52–60.
https://doi.org/10.32972/dms.2024.005

THE EVOLUTION OF PRINTING: A JOURNEY OF TECHNOLOGICAL AND SOCIAL PROGRESS

[1]MADDALENA PIZZEGHELLO – [2]FERENC SARKA

[1]University of Genova, Via Opera Pia 15, 16145 Genova, Italy
[2]University of Miskolc, Institute of Machine and Product Design
H-3515, Miskolc-Egyetemváros
[1]maddypizzeghello@gmail.com, [2]ferenc.sarka@uni-miskolc.hu
[2]https://orcid.org/0000-0003-3136-4248

Abstract: The history of printing is a captivating narrative that has significantly influenced the dissemination of knowledge and the development of human society. This article explores the prehistory of literacy, the emergence of writing systems, the tools used before the invention of printing, and the profound impact of Johannes Gutenberg's movable type printing press. It also discusses the challenges faced by printing technology over the centuries, the role of digitalization, and the enduring value of traditional printing.

keywords: *ancient writing, papyrus, Guttenberg, stencils, hieroglyphs, primitive methods, printing presses, modern printing technologies*

1. INTRODUCTION

The history of printing is a fascinating journey that has had a profound impact on the spread of knowledge and the development of human society. From its earliest beginnings in ancient times, the art of reproducing written materials has undergone remarkable transformations, paving the way for the information age we live in today (Britannica Encyclopedia, 1974).

The origins of printing can be traced back to the human desire to preserve and share information. In ancient civilizations, various methods were employed to reproduce texts and images, although on a smaller scale compared to the advancements that would come later. These early techniques laid the foundation for the revolutionary innovations that would shape the future of printing (Mayor, 1980).

One such method was the use of seals and stamps to create impressions on different surfaces. In ancient societies, individuals would carve intricate designs or symbols onto stone, clay, or other materials. These seals could then be pressed onto wet clay, wax, or other soft substances, leaving behind an impression that replicated the original design. This technique allowed for the duplication of important documents and messages.

Another method that emerged in the ancient world was the use of stencils. By cutting or perforating patterns or characters into materials such as leaves or bark, individuals could create templates for reproducing texts or images. Ink or dye could be applied over the stencil, resulting in the transfer of the design onto another surface.

Additionally, some ancient cultures explored the use of relief techniques. For instance, in ancient Egypt, artisans would carve hieroglyphs or pictorial representations onto stone or clay tablets. These tablets could then be used to create moulds, into which molten metal or other materials were poured. Once cooled, these moulds would yield replicas of the original inscriptions. While these early printing techniques were limited in terms of scale and complexity, they marked the beginnings of a journey that would ultimately revolutionize the dissemination of information.

In effect by examining the early stages of printing history, we gain a deeper understanding of the remarkable progress that has shaped the world of printed communication. From the primitive methods of seals, stencils, and relief techniques to the transformative innovations that have driven the print industry forward, the history of printing is a testament to human creativity, curiosity, and the enduring quest to share knowledge with others. The subsequent chapters will delve into the advancements that followed, exploring the development of movable type, the impact of printing presses, and the emergence of modern printing technologies (Britannica Encyclopedia, 1974).

2. PREHISTORY OF LITERACY AND SPREAD OF WRITING

In the early stages of human history, literacy did not exist as we know it today. The earliest forms of written communication date back over 5,000 years ago with the invention of cuneiform writing in Mesopotamia (Figure 1., a) and hieroglyphic writing (Figure 2., b) in Egypt. These early forms of writing were primarily used for administrative, religious, and commercial purposes.

Humanity abandoned the nomadic lifestyle and settled down. Ancient civilizations were formed. They were formed in trade using money as means of exchange. In order to operate the social system, it was necessary to have some means by which expenses and income could be tracked. This tool became writing (not only letters but also numbers) (Wright, 2015).

These writing systems were engraved on clay tablets using a wedge-shaped stylus and was mainly used for administrative and commercial purposes. In those old days, the direction of writing and reading was not yet accepted. We find mixed writing from right to left, from left to right, and even from top to bottom. Even today it is not completely uniform (Arabic and Hebrew write from right to left). The language of the old days was often forgotten and deciphering them posed/remains great challenges for today. Many times, a finding that does not seem very significant at first provides give us the solution to deciphering the language, like in the case of Rosetta stone.

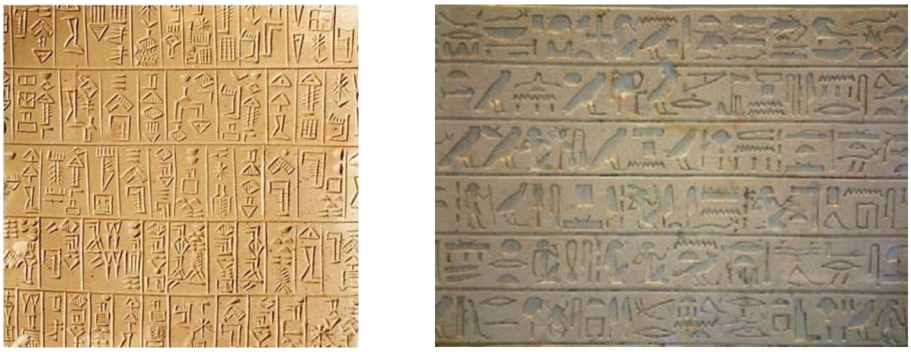

a) b)

Figure 1. *a) Sumerian writing b) Egyptian hieroglyphs*

a) https://hu.wikipedia.org/wiki/%C3%89k%C3%ADr%C3%A1s
b) https://en.wikipedia.org/wiki/Punchcutting

During prehistory, the earliest forms of written communication consisted of symbols and images that represented specific objects and concepts. Over the centuries, writing has developed in different parts of the world. In Egypt, for example, the hieroglyphic writing system developed, which used symbols and images to represent words and concepts. The alphabet, as we know it today, was developed by the ancient Phoenicians around 1200 BC and later adopted by other cultures, including the Greeks and Romans (Robinson, 2009).

2. 1. Support documents and tools before printing

Before the invention of printing, written documents were made on a variety of materials, such as papyrus in Egypt, parchments made of animal skin in the Roman Empire, and scrolls of silk or paper in China. These materials required a specific preparation process before they could be written. For example, animal skin had to be treated and smoothed to create a surface suitable for writing (Fig. 2.).

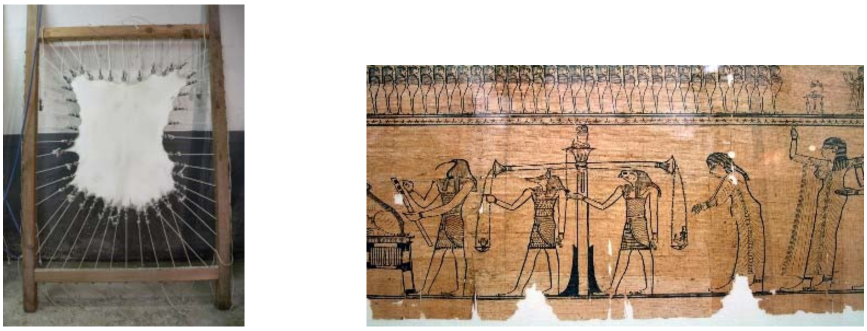

a) b)

Figure 2. *a) Parchment Preparation (a goat skin stretched and dried on a frame) b) Detail from the book of the dead of Taruma, 3rd to 2nd century BC*

a) https://blogs.cornell.edu/culconservation/2015/04/03/parchment-making/
b) https://it.wikipedia.org/wiki/Papiro

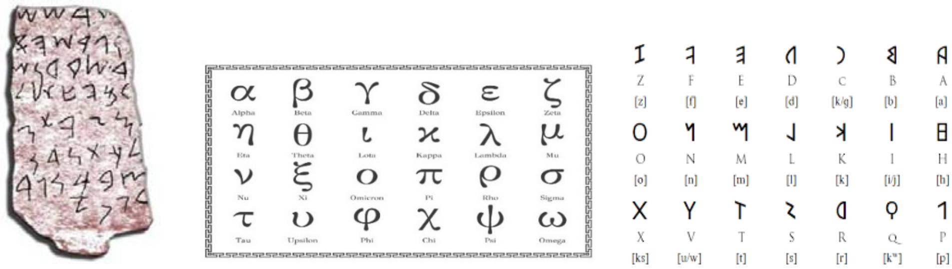

a) b) c)

Figure 3. *a) Phoenician alphabet b) Greek alphabet c) The Old Turkic alphabet*

a) and b) https://it.wikipedia.org/wiki/Alfabeto_fenicio
c) (Scharlipp, 2000)

2. 2. Beginning of literacy and the reason for it

The beginning of literacy, as we know it today, can be attributed to the ancient Phoenician civilization around 1200 BC. The Phoenicians developed a writing system (Figure 3. a)) based on an alphabet composed of 22 consonants. This alphabet later influenced the development of other writing systems, such as the Greek

(Figure 3. b)) and Latin (Figure 3. c)) alphabets. Literacy had a significant impact on the spread of knowledge, as the alphabet made learning to write easier than previous writing systems based on complex symbols (https://en.wikipedia.org/wiki/Literacy).

2. 3. Egypt, Roman Empire, China, medieval codices, codex copyists (monks)

Egypt is known for its hieroglyphic writing system used to record history, religion and administration. In the Roman Empire, parchments were used for official documents and literature. In China, woodblock printing was an early form of printing that enabled the production of religious and literary texts (Dixon, 2006).

a)

b)

Figure 4. *a) Facsimile of the Dresden Codex 13th or 14th century made in the Yucatan Peninsula, Mexico, b) Early Medieval Art*

a) https://blogs.getty.edu/iris/explore-a-global-middle-ages-through-the-pages-of-decorated-books/
b) https://it.wikipedia.org/wiki/Cassiodoro

During the Middle Ages, Christian monks played a crucial role in manually copying sacred and literary texts (Figure 4.), thus preserving knowledge during a period of political and economic instability. In fact, the production of written documents before the invention of the printing press required a large amount of time and resources. Texts were copied by hand by scribes or copyists, the production of books therefore required considerable effort and the volumes were generally reserved for a few privileged people (Britannica Encyclopedia, 1974).

3. Combination of technologies needed for Gutenberg

The invention of movable type printing, attributed to Johannes Gutenberg (Figure 5) in the 15th century, marked a turning point in the history of the diffusion of ideas. Birth date of Gutenberg is not known, he was born around 1400 in Mainz. He started his carrier as metal worker, goldsmith and mirror maker. Mirror-making did not go well, so he looked for something new to help him get out of financial problems. Gutenberg combined several existing technologies to create an efficient movable type printing press. The metal industry was needed to produce movable metal type, metalworking to create sturdy and precise printing machines, and the paper industry to provide a suitable printing medium.

In Guttenberg's time, printing presses and printing clichés already existed. These contained images of the text of an entire page at the same time, so changing the text or creating a new text was very difficult. Starting from this problem, Guttenberg broke the text of the page into letters. From these, any text could easily be put together quickly. Printing clichés that can be assembled letter by letter have been in use for centuries in the Chinese Empire, but they were made of wood. In contrast, Gutenberg already used metal letters. Gutenberg experimented with the so-called type of metal (lead 50–86%, antimony 11–30% and tin 3–20%.), which was quite soft, and the paint adhered to its surface properly. Additionally, Gutenberg developed an oil-based ink that adhered to movable type and allowed for crisp, consistent printing. For each letter, he developed a "master" piece made of steel.

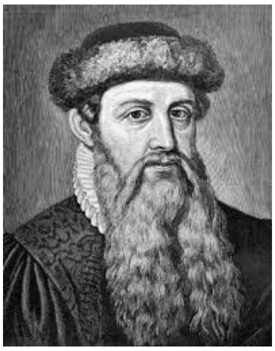

a)

b)

Figure 5. a) Johannes Gutenberg
b) Johannes Gutenberg with his printing press

a) (Britannica Encyclopedia, 1974)
b) https://commons.wikimedia.org/wiki/File:Gr.diana_Johannes_Gutenberg.png

This master letter was punched into a metal plate, and the type of metal was casted into the depression that appeared in the metal plate. Thus, the ruined letters could be reconstructed. Since the letters were made of metal, they could be manufactured more precisely, thus the distance between the letters and the distance between the

lines of text could be kept very precisely. It can be concluded that Gutenberg's genius lay in the fact that he combined existing technological elements into a new technology, for which we are known today as the "father of book printing" (Britannica Encyclopedia, 1974).
The invention of movable type printing, attributed to Johannes Gutenberg in the 15th century, marked a turning point in the history of the diffusion of ideas. His movable type printing press allowed texts to be quickly composed and multiple copies of the same document to be produced in much shorter times than manual copying. This invention has indeed had a revolutionary impact on the diffusion of knowledge. Books and other documents could be produced in larger quantities and at lower costs, making reading and literacy accessible to a wider audience. The press contributed to the Renaissance and the Protestant Reformation, spread ideas and favoured the spread of scientific and philosophical knowledge.

4. Characteristic of Printing Presses and Emerging Problems

Gutenberg's first movable type printing presses consisted of a manually operated wooden press. These machines allowed composing texts quicky by composing and positioning movable type. However, there were still some technical challenges, such as the need for a complete set of characters for each page and the difficulty of maintaining uniform pressure when printing.
Johannes Gutenberg's most famous and influential work was the printing of the Bible, commonly known as the Gutenberg Bible. This monumental achievement marked the beginning of the mass production of books through movable type printing. However, it's worth noting that during that time, the ink and paper used in printing were not always healthy. The ink contained high levels of lead, which posed a risk to the health of the printers and readers. Additionally, the paper used in early printed books was often made from linen rags, which were treated with various chemicals to achieve a smoother surface for printing. These chemicals, such as alum, could be toxic. As a result, some of these early books are now considered hazardous and require special handling. In old libraries, you may find books where pages can only be turned with gloves to protect against the toxic substances present (Moran, 1971).
Throughout the centuries, various improvements were made to overcome technical challenges in printing presses. Mechanical printing increased production speed and ensured more uniform pressure. Innovations like cylinders, inclined planes, and water-based inks further enhanced the printing surface, ease of cleaning, and allowed for a greater variety of colours. Modern printing techniques, including screen

printing and microincision coating, continue to advance the production of high-quality and complex printed materials.

In modern printing machines, speed control is a crucial aspect to ensure smooth and precise printing. The speed of the printing machine's rollers, which feed the paper through the press, needs to be carefully regulated. If the speed is not controlled properly, various issues can occur. For example, if the rollers have different diameters and rotate at inconsistent speeds, the paper may tear or buckle. Additionally, if the axles of the rollers are not parallel, the paper may slip off the rollers, leading to misalignment and poor print quality. To address these challenges, sophisticated systems have been developed. Safety chucks, pneumatic shafts, and compensator parts are examples of solutions used in the industry. Companies like Montalvo and IBD Wickel Technik specialize in providing advanced technologies for speed control and tension control in printing processes, ensuring smooth and reliable operation (Hanson).

The invention of the printing press had a transformative impact on human society. Books and printed materials became faster and cheaper to produce, leading to greater dissemination of knowledge, democratization of information, and increased literacy. The printing press played a crucial role in the spread of ideas during the Enlightenment and the Protestant Reformation (around 15^{th} century) (https://courses.lumenlearning.com/suny-massmedia/chapter/4-2-history-of-newspapers/).

Printing technology has continuously evolved from Gutenberg's movable type printing to lithographic printing, rotary printing, and digital printing. Digital printing has introduced new possibilities, such as on-demand production, personalization, and rapid dissemination through digital means. Printing technology has overcome challenges related to precision, speed, and quality of the final product. Today, printing encompasses a wide range of materials, from traditional books and newspapers to metal surfaces, plastics, fabrics, and even printed circuit boards.

5. The impact of digitalization on printing

With the appearance of digitalization, traditional printing has faced new challenges. The accessibility of digital content and online dissemination has reduced the demand for traditional printed materials like newspapers and magazines. However, printing continues to play a vital role in academic publishing, the production of promotional materials, and fine art printing. Traditional printing retains its charm and value, offering a tangible and authentic experience that differs from digital devices. Books and printed materials provide a unique reading experience, fostering emotional connections with the content.

6. Summary, conclusion

The evolution of printing from its early beginnings to modern times has had a profound impact on human society. From the prehistory of literacy to the invention of Gutenberg's printing press, the spread of knowledge, literacy, and ideas has been accelerated and democratized. Printing technology has constantly overcome technical challenges, adapting to new materials, inks, and processes to produce high-quality printed materials. While digitalization has brought new opportunities and challenges to the printing industry, traditional printing continues to hold its value, offering a tangible and authentic experience that resonates with readers and consumers. As technology continues to advance, the printing industry will undoubtedly adapt and innovate, ensuring its continued relevance in the ever-changing landscape of communication and knowledge dissemination.

References

Britannica Encyclopedia (15th ed., Vol. 29). (1974). Encyclopaedia Britannica (UK) Ltd.

Dixon, H. (2006). 33. Manuscripts. *The Edinburgh Companion to Ancient Greece and Rome*, 251-261. doi:https://doi.org/10.1515/9780748627141-039

Hanson, E. (n.d.). How a Printing Press Works. Retrieved from https://www.imaging.org/IST/IST/Resources/Tutorials/Printing_Press.aspx

Mayor, A. (1980). *Prints and People: A Social History of Printed Pictures.* Princeton University Press.

Moran, J. (1971). The Development of the Printing Press. *Journal of the Royal Society of Arts, 119*, 281-293.

Robinson, A. (2009). *Writing and Script: A Very Short Introduction* (1st ed.). Oxford University Press. doi:https://doi.org/10.1093/actrade/9780199567782.001.0001

Scharlipp, W. (2000). *An Introduction to the Old Turkish Runic Inscriptions.* Engelschoff: Verlag auf dem Ruffel.

Wright, J. (2015). *International Encyclopedia of the Social & Behavioral Sciences* (2nd ed.). (J. Wright, Ed.)

Design of Machines and Structures, Vol. 14, No. 1 (2024), pp. 61–74.
https://doi.org/10.32972/dms.2024.006

RESEARCHING THE GEOMETRIC LIMITS OF 3D LASER SCANNING

FERENC SARKA[1] – ANDRÁS MALIK[2]

[1]*University of Miskolc, Institute of Machine and Product Design*
H-3515, Miskolc-Egyetemváros
[2]*Schaeffler Automotive GmbH & Co. KG, Bühl, Germany*
[1]*ferenc.sarka@uni-miskolc.hu,* [2]*malikandras@gmail.com*
[1]*https://orcid.org/0000-0003-3136-4248*

Abstract: The paper presents the geometrical properties of those surfaces that can be digitized by 3D laser scanners. First the circumstances of the experiment are described. The device (Roland LPX-1200) and applied software (Dr. Pizza) are also introduced, such as the brief historical development of 3D digitization. Based on the data found in the literature, all those problems are collected, that can emerge during 3D laser scanning. In order to find the limits of the scanner, a test specimen was designed with a variety of geometric elements (planes in different positions, curved surfaces (concave, convex), roundings and chamfers in different sizes and positions, holes of different depths and diameter). During the design of the test specimen, those properties that were developed for additive technologies were used. The test specimen was produced by milling technology (Roland MDX 650), and then scanning with different settings were performed on it. The experiment was carried out until the largest real surface was digitized. Based on the test, it was summarized which geometries can be fully or partially scanned. Finally, a recommendation to achieve the best possible result was formulated.

Keywords: *3D scanning, laser scanning, scannable geometry, test piece for 3D scanning.*

1. INTRODUCTION

3D scanning, or digitization, occupies an increasingly large part of today's engineering practice. With the spread of various 3D technologies (3D printing, CAxx technologies), digitalization technologies have also developed. The market for 3D scanners is huge, ranging from hobby-level devices to special-purpose devices worth tens of thousands (EUR). Their field of use is very broad, whether it is for civil or military applications. It can be used in almost every part of the natural science field, be it mechanical engineering, archeology, architecture, art, or even medical (MRI, ultrasound). In the present paper, the use for mechanical engineering purposes of 3D scanning is introduced, during which those geometric limits that are still suitable for digitization were looked for.

Research on the topic was started on the basis of an assignment from an industrial partner. It became necessary to replace and reproduce a plastic injection moulded part. During the scanning of the part, we observed geometric surfaces that the laser scanner could not digitize (Figure 1). Based on the experience gained, we realized that it would be worth to examine the problematic geometries in a controlled manner.

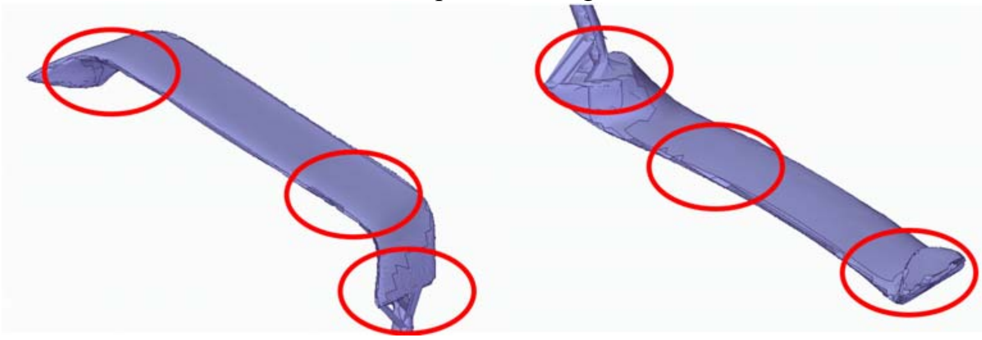

Figure 1. *Image of the part the research started with (Solid Edge 2020)*

Figure 1 shows that the model created by the scanner is incorrect in several places, non-existent surfaces were included, and existing surface parts were not digitized. Most of the problems were at the junction of the surfaces and at the edges.

2. The history of the 3D scanner – in brief

The production/reconstruction of bodies in sculpture appeared already in ancient times and artists used different techniques to create a sculpture based on a model or the original body (Sargentis, et al., 2022). In practice, the techniques of the time were the forerunners of scanning and printing. The first optical recording of geometry dates from 1859 (Sobieszek, 1980). François Willème patented a process he called photosculpture. During the procedure, he took 24 pictures of the object, every 15 degrees along a circle (Figure 2).

Based on the 24 images, he recorded the contour of the body, then displayed the profile using a pantograph milling machine. By placing the 24 profiles in the correct position, you get a (fairly rough) optical copy of the original body. Of course, a real sculptor was also needed to complete the final result. Willème was originally a sculptor, so the ability was available. The technological development of scanning was given a big boost by the development of computer technology and its ever-lower price. The first scanners appeared in the early 1960s, these systems used light, cameras and projectors. The shape of the surface was recalculated from the distortion of the image (structured light) projected onto the body. Scanners operating on this principle are still available today, called optical scanners (Edl, Mizerák, & Trojan, 2018), (Sarka & Szente, 2011), (Kristály & Ficzere, 2021b). The use of laser light (discovered by Hughes in 1960) for recording the geometry of bodies only appeared in the 1990s. Even this date represents 30 years of development and experience up to the present day. The scanner used in the presented research was manufactured in the 2010s. The scanner used is a non-contact, surface digitizing device, which determines the points of the surface using a laser beam. The control software creates a point cloud from the measured data, from which it generates a surface. It determines the points based on the reflection of the emitted laser beam into the sensor. The device measures the time between the start and arrival of the emitted laser beam, determines the distance of the given point based on the speed of the beam (spot-beam triangulation). The process is easy to understand based on Figure 3.

Figure 2. *The photosculpture (Edl, Mizerák, & Trojan, 2018)*

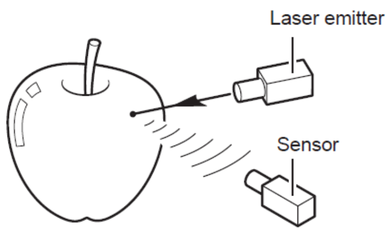

Figure 3. *Operating principle of the laser scanner*

LPX-1200 User's Manual, Roland DG Corporation

3. PRESENTATION OF THE DEVICE USED

For scanning, LPX-1200 type laser scanner from Roland DG was used, which was purchased at the Institute in 2011. The scanner is shown in Figure 4. The scanner can operate in two modes, rotary and planar. In the case of rotary scanning, the specimen table rotates while the source of the laser beam moves vertically. In the case of planar, both the beam source and the specimen table move, but only at an angle of +- 20° relative to a specific vertical plane. The smallest value of the resolution is 0.1 mm. The device can scan components with a size of Ø130 mm x 203.2 mm (5 inch x 8 inch).

Figure 4. *Image of the applied device*

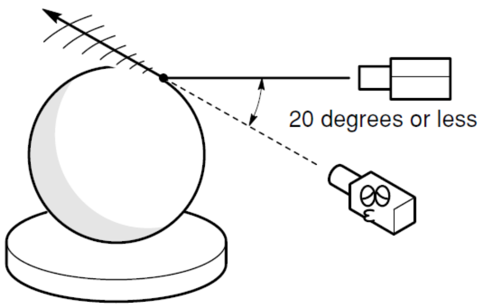

Figure 5. *The laser beam arriving at a low angle is not reflected, but "travels further"*

LPX-1200 User's Manual, Roland DG Corporation

Instructions of the device draw attention to some problems at the very beginning, that may occur during body scanning.

- The body-surface where the laser beam hits the body cannot be scanned at a low angle. Enter this angle as 20°. Figure 5 shows why is this problem almost unavoidable. Each body come to an end somehow, so we are bound to encounter problems at the top and bottom of the parts.
- Relatively smooth surfaces can be scanned well, while fabrics or bodies with very rough surfaces cannot be scanned.
- There are objects that cannot be scanned due to their material, such as transparent or translucent materials. In these cases, the laser beam passes through them without being reflected.
- The colour of the objects also affects the result of the digitization. The colours black and dark blue absorb the light of the laser beam, so that no light is reflected from the surface of the objects to the sensor.
- A similar problem was experienced with shiny and reflective surfaces, regardless of the colour of the object. In case of objects like this, the laser beam is scattered and does not return to the sensor.
- There were also suggestions for how to place the objects on the specimen table, the most important of which is to place the objects in the centre of the table if possible.
- If an object with a hole (with a bore) has to be scanned, the object should be placed in such a position that the laser beam has the opportunity to pass through the hole (bore).

Even if the listed conditions are met, there is no guarantee that the result will be good. This was exactly experienced during the task described in the Introduction. That is why additional problematic geometries were looking for. With the help of a specimen developed for the test grouping and organizing of the revealed geometries were in the focus of the further research.

4. SEARCH FOR TEST PART

Before the test part was designed, a literature survey was carried out to see if anyone else had a similar problem. Several test bodies with hair-raising shapes were found. After reading the description of these models, most of them are used for testing 3D printers. Some of them are shown in Figure 6**Hiba! A hivatkozási forrás nem található.**.

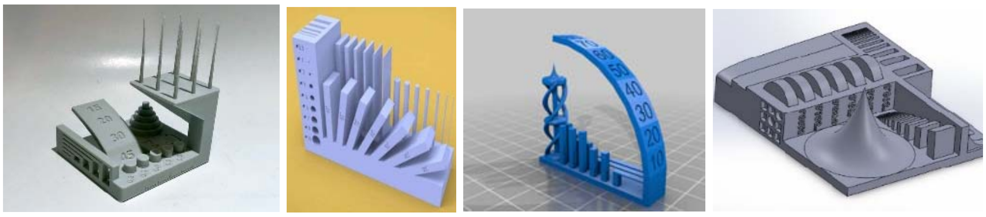

Figure 6. *Various test bodies*

https://www.printables.com/
https://3dmatic.com.au/download/3d-printing-test/
https://creazilla.com/nodes/7836086-3d-printer-tolerance-test-3d-model

Based on the research, and on the authors own thoughts the following functions were determined:

- Curved surface parts: convex surfaces (different sizes) and concave surfaces (in different sizes).
- Flat surface parts: placed at different angles to the base plane, or undercut, recurved surfaces.
- Holes, depressions with different diameters, or/and with different depth.

The properties of the scanners are determined by several metrics, so the test specimen also must have such properties that the limits of these metrics can be stretched. During the research, we found several metrics that can be affect the quality of scanning.

- Resolution: x, y, z, coordinates, in case of planar scanning, and degree and z coordinate in case of rotary scanning.
- Depth of Field (DOF): in the case of optical scanners, the distance at which a sharp structured image can still be projected onto the body.
- Accuracy: the difference between the scanned and the real body.

Since the revealed test parts support the examination of the quality of 3D printing, the test specimen was started to be designed. When designing it, the main focus was on all the suspected problematic geometries could be inserted into the same part.

Based on previous scanning experiments, problematic geometries should be understood as chamfers, roundings, edges, smaller or larger depressions, and planes located in a certain direction compared to the scanner's base plane.

For chamfers and roundings, a variable amount of edge-modifications were created, so that the size that the scanner can still digitize could be found. The edge modification is between two flat surfaces, which are 90 degrees in relation to each other in the first approach (in a later experiment, the extent to which the angle closed between the edges affects the scanning result will also be examined). To make the holes scannable, holes of variable diameter and depth must be created.

5. The designed specimen

In addition to taking into account the above aspects, the technology of its production must also be taken into account when designing the planned test specimen. In the case of forming by cutting, on the bordering surfaces a draft was applied. In this case that part of the machining tool where there is no cutting edge does not rub against the workpiece. Figure 7 shows the CAD model of the specimen and the different geometries marked from A to J.

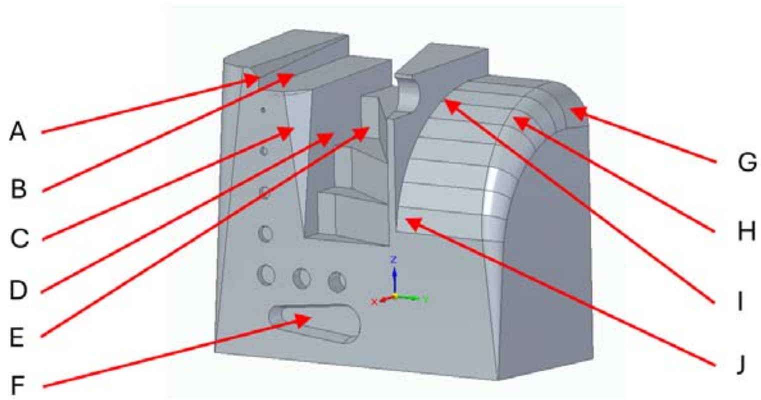

Figure 7. *The designed specimen and the various surface parts*

Geometries:
A: Rounding with variable radius.
B: Chamfer with variable size in the direction of scanning.
C: Holes of different diameters and depths.
D: Chamfer of variable size perpendicular to the scanning direction.
E: Flat surface parallel to the scanning direction.
F: Conical surfaces of different sizes.
G: Rounding with a variable radius, between surfaces with different angles.
H: Planes subtending different angles with the scanning direction (every 10 degrees).
I: Concave, curved surface with variable width.
J: Planes subtending different angles with the scanning direction.

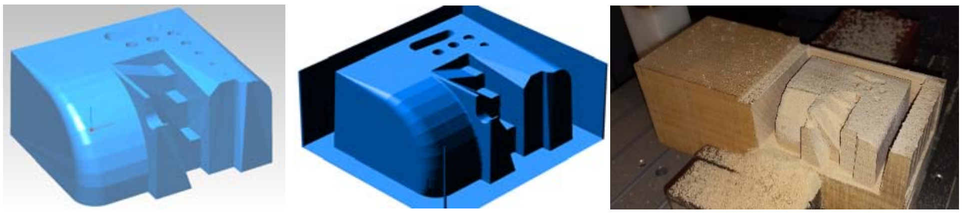

Figure 8. *The model is in the software of the milling machine, in the simulation program, and then during production (from left to right)*

It would be obvious to use 3D printers to produce the test piece, but in order to the specimen to be as precise, as a standard or a tool, it was produced by traditional cutting technology. Cutting is done with a Roland MDX-650 prototype milling machine. Before cutting, a simulation was carried out (Figure 8) to determine which tool size is capable to perform the cutting operation. The simulation was performed with the software included with the Roland machine (Modella Player and Virtual Modella). The vast majority of the formed surfaces can be created with a straight-edged tool with a diameter of 3 mm (Figure 8). Small holes were produced later by drilling. The test specimen was made of steamed beech material. The test specimen (Figure 9) was cut out of the raw material and performing some minor grinding operations.

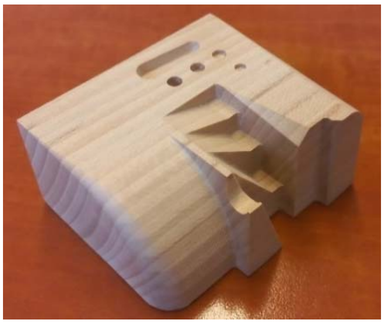

Figure 9. *The finished test specimen*

6. Structure and presentation of the study

Possible operation modes of the scanner were used as a basis for the structure of the test series. When introducing the scanner, it was already mentioned that the scanner can operate in two modes (rotary, planar). In the case of plane scanning, it is possible to enter several planes (maximum of six). In both operating modes, it is possible to change the resolution. Based on these, the following list was compiled:

- Rotary scanning at 180 degrees, with a resolution of 1 mm.
- Rotary scanning at 180 degrees, with a resolution of 0.5 mm.
- Planar scanning, 1 plane, with two resolutions. The plane is parallel to the front surface of the workpiece.
- Planar scanning, 2 planes, 30 degrees relative to each other (one rotated to 15 degrees, the other to -15 degrees.
- Planar scanning, 3 planes, 40 degrees relative to each other (one rotated to 40 degrees, the other to -40 degrees, the third stayed in 0 degree position.

The specimen was placed in the centre of the specimen table. Fixing plastic provided by Roland was used to fix the specimen in its position. Figure 10 – Figure 15 show the results of the scanning.

Rotary scanning

In the first approach, the rotary scanning option was chosen. The specimen was placed in the centre of the table as recommended. The scan was made with two different resolutions (circumferential pitch: 0.9 and 0.4 degree, height direction pitch 1 mm and 0.5 mm) (Figure 10).

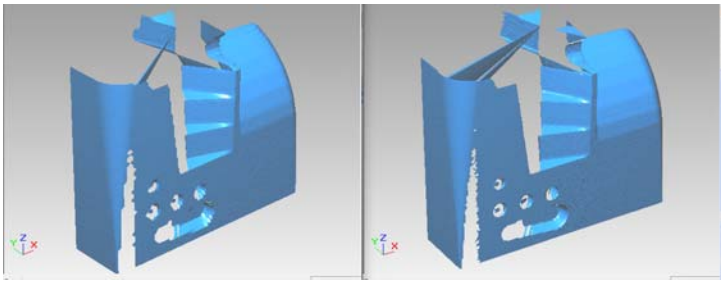

Figure 10. *The result of the rotary scan in two resolutions*

There is no change in the size of the digitized surface, but the surface detail has improved. Based on this, it can be stated that the resolution has no effect on the size of the scanned surface, only its quality. In the next step, the body was placed closer to the source of the laser beam, as close as the table could allow. The resolution remained the same as in the previous case. The result can be seen in Figure 11. The image on the left is the result when the specimen was placed in the centre of the specimen table, the image on the right is the result when the specimen was placed on the edge of the specimen table. With this, all the possibilities inherent in the rotary scanning option were exploited. The result is not satisfying.

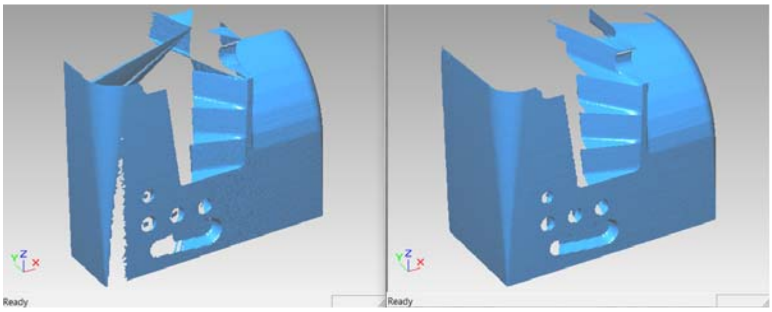

Figure 11. *Image of the test specimen placed in the centre and the test specimen placed on the edge*

Planar scanning

After that, the planar scanning option was switched. The first test option was one plain scan. The resolution is 1 mm. A comparison of the results can be seen in Figure 12.

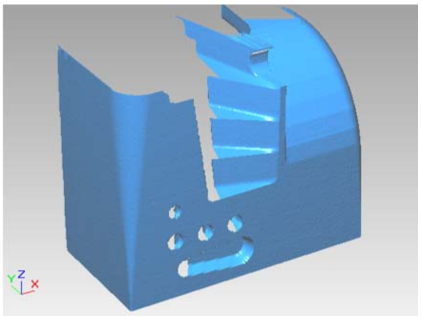

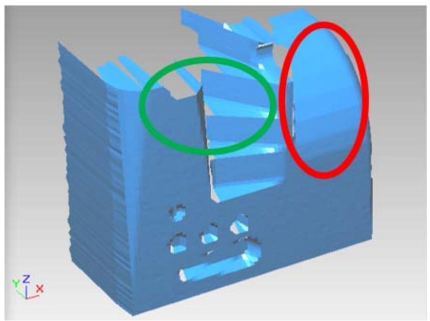

rotary planar

Figure 12. *The result of planar scanning compared to rotary scanning*

The specimen remained in a position close to the radiation source. More of certain parts of the surface managed to be digitized (green), but some parts were lost (red). The direction is promising, but the surface of the specimen is still not known.

Continuing the work, the number of scanning planes were increased. First, 2 planes were activated. There was a 30° difference between the planes (+15° – -15°). The surface got much better, but the quality is still not good enough (Figure 13).

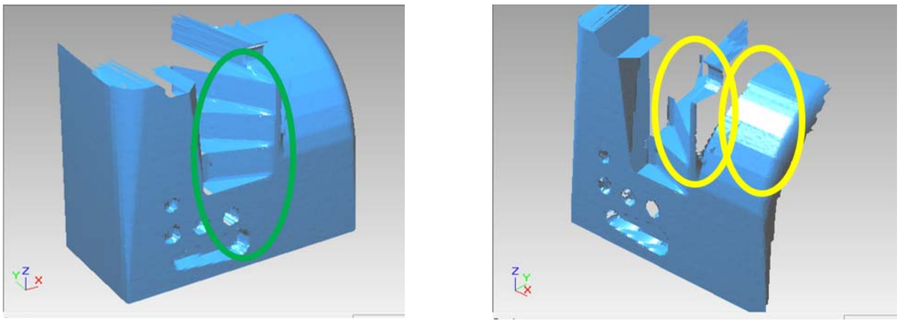

Figure 13. *The result when using two scanning planes*

Based on the above mentioned, scanning those planes that are parallel to the direction of the source of the laser beam is difficult. The further the specimen is from the source, the more uncertain the result is. Next another plane was introduced, so scanning takes place from three directions. The goal is to explore the limits of the machine. If the scanned surface that cannot be created better with the machine is found, then it can be determined which geometries mean a problem for the laser scanner. The three planes were located at -40°, 0°, +40°. Figure 14 shows the results.

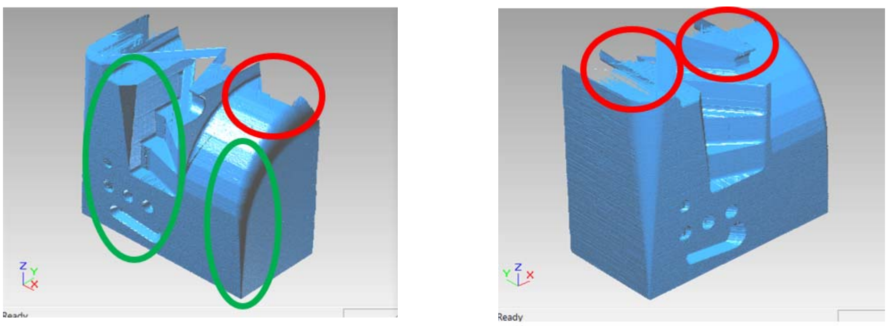

Figure 14. *The result of scanning in three planes, viewed from two directions*

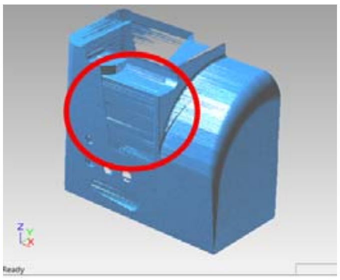

Figure 15. *The result when 3 planes are used, the planes are 90° apart*

In the left image of Figure 14, the significant increase of the scanned surface is clearly visible. This is because of the use of the new scanning plane. However, there are still parts of the surface that are not visible for the scanner (marked with red in Figure 14, and there are also surface elements that are not existing on the real specimen. These can be removed from the model with meticulous work, but that way the primary purpose of scanning would be lost. From the test, it can be deduced that surfaces parallel to the direction of scanning laser beam and at an angle smaller than 10° cannot be scanned. This is a favourable result as the factory description gave 20° for this value. During the test, the angle between the scanning planes was further increased to 90 degrees, the result can be seen in Figure 15. A lot of unreal surfaces have already appeared here, this model can no longer be used even with manual modifications. The last test was already well beyond the limit that would still result an acceptable model.

7. Application of surface coating

After the scanning experiments, the change in the surface structure of the test specimen and its effect on the scanning result were examined. For this we used a primer (Mr. Hobby, MrFinishing Surfacer 1500, white) as it can be seen in Figure 16. The paint was applied to the surface of the specimen with an airbrush gun, approximately 60 µm thick, applied in 3 layers. This operation is not allowed in all cases. On the one hand, the real dimensions of the part are modified, on the other hand, it is not possible to apply paint to a shaped surface at a constant thickness, so the change in size will not be uniform. Removing the paint is not easy, it is often impossible without damaging the original part.

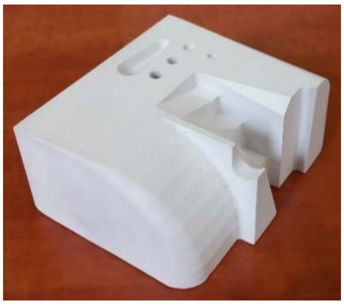

Figure 16. *The painted specimen*

The use of white matte paint slightly improved the result (Figure 17), but there are still many surfaces that are incorrect, have not been digitized, or simply do not exist. In the case of a component with a shiny, glossy surface, matting is essential, but no significant improvement can be achieved on the original matt surface of steamed beech.

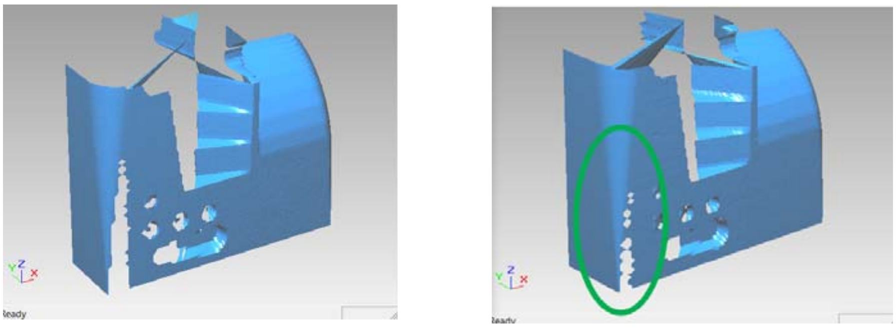

Figure 17. *Comparison of the scanned results of painted and unpainted parts*

8. Summary of results

The size of the surfaces recognized by the laser scanner depends on the relative position of the radiation source and the object. In the study, the body placed closer to the source gave better results, both in case of rounding and chamfering.

The data found in the literature, according to which the laser beam must form an angle greater than 20 degrees with the scanned surface, can be changed to the fact that it must form an angle greater than 10 degrees. Surfaces parallel to the direction of the laser beam cannot be scanned at all. If the depth of the holes is greater than 1 mm, it cannot be scanned.

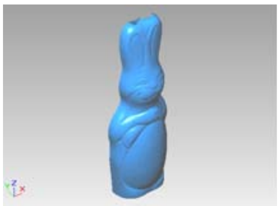

Figure 18. *Model of a hollow chocolate figure*

Based on the series of experiments, it can be concluded that the geometries that are common in technical practice, usually built from basic bodies (cylinders, columns, planes, etc.) can be digitized less satisfying with the help of a laser scanner. On the other hand, sculptural, relief-like bodies with not too large depressions and a matte white surface can be easily scanned. Figure 18. shows a gypsum model of a hollow chocolate figure. The scanning is almost perfect, except for the upper peak, where the laser beam hit the body at an angle of less than 10 degrees.

REFERENCES

Edl, M., Mizerák, M., & Trojan, J. (2018). 3D laser scanners: history and applications. *Acta Simulatio, 4*(4), 1-5. doi:https://doi.org/10.22306/asim.v4i4.54

Kristály, Á., & Ficzere, P. (2021a). Utilization of 3D Printing in Replacement of Basic Plastic Workpieces. *International Journal of Engineering and Management Sciences, 6*(2), 274-282. doi:https://doi.org/10.21791/IJEMS.2021.2.24.

Kristály, Á., & Ficzere, P. (2021b). Study on the Photo-Based 3d Scanning Process. *Hungarian Journal of Industry and Chemistry, 49*(2), 15-18. doi:https://doi.org/10.22306/asim.v4i4.54

Sargentis, G.-F., Frangedaki, E., Chiotinis, M., Koutsoyiannis, D., Camarinopoulos, S., Camarinopoulos, A., & Lagaros, N. (2022). 3D Scanning/Printing: A Technological Stride in Sculpture. *Technologies, 10*(1), 9. doi:https://doi.org/10.3390/technologies10010009

Sarka, F., & Szente, J. (2011). *Interaktivitás a tervezésben és a prototípusgyártásban.* Budapest: Nemzeti Tankönyvkiadó.

Sobieszek, R. (1980). Sculpture as the Sum of its Profiles: François Willème and Photosculpture in France. *The Art Bulletin, 62*, 617-630.

Design of Machines and Structures, Vol. 14, No. 1 (2024), pp. 75–83.
https://doi.org/10.32972/dms.2024.007

OPTIMIZATION OF MULTI-CRITERIA DECISION-MAKING FOR DENTAL IMPLANT SELECTION

JUDIT ALBERT[1] – ÁGNES TAKÁCS[2]

University of Miskolc, Institute of Machine and Product Design
H-3515, Miskolc-Egyetemváros
[1]szalai.judit@student.uni-miskolc.hu, [2]takacs.agnes@uni-miskolc.hu
[1]https://orcid.org/0000-0001-8043-5503, [2]https://orcid.org/0000-0002-3210-6964

Abstract: The long-term biomechanical performance of dental implants is significantly influenced by material composition, anticipated loads, and the geometry of the interface between the implant and the bone. This study applies multi-criteria decision-making methods to select an optimal construction strategy. Through finite element analysis, variables such as implant geometry and stress distribution during loading are integrated into the decision-making process. By processing the results of alternative implants, we ranked these alternatives using an Excel implementation of the VIKOR decision support method commonly used in the literature. Results indicate that the optimal stress distribution depends on the size and shape of the implant. Selecting symmetric fixation points and optimal distances may enhance implant stability and long-term performance.

Keywords: *Multi-criteria decision making, VIKOR method, dental implant*

1. INTRODUCTION

MCDM (Multi-Criteria Decision Making) is a decision-making method that helps reconcile different, often conflicting conditions in the decision-making process. Through the application of MCDM, decision-makers can:

- ***Consider multiple factors:*** MCDM allows decision-makers to simultaneously consider various factors. For instance, in the case of implants, this could include factors such as elastic modulus, antimicrobial properties, support for osteogenesis, etc.
- ***Prioritize:*** MCDM enables the prioritization of different factors in the decision-making process, determining which are the most important or prominent.

- ***Compare alternatives:*** MCDM facilitates the objective comparison of alternatives, taking into account all relevant factors.
- ***Sensitivity analysis:*** MCDM helps assess the sensitivity of results to different factor weightings or alternative selections.

In this case, MCDM assists decision-makers in comprehensively examining the advantages and disadvantages of different models for implants and properly aligning them with given conditions. Through the application of MCDM, decision-makers can better prepare to make optimal decisions among conflicting conditions, considering and weighting different criteria and constraints, such as implant fit, material, fixation, and cost-effectiveness, already in the design process. Consequently, well-founded and balanced decisions can be made for the best fixation construction alternatives in implant design, ensuring the best possible outcomes for patients.

Ideally, optimal fixation construction alternatives should result in minimal stress concentration, evenly distributing external loads onto connected bones. Therefore, the primary goal is to achieve optimal deformation, ensuring compatibility with external loading conditions. Key to this is identifying critical parameters with the greatest impact on implant deformation. We examined mechanical stresses arising in implants and deformations, focusing on three implant alternatives. Finite element analysis of implant mechanical properties was conducted for Ti-6Al-4V material. The Ti-6Al-4V exhibits greater resistance to deformation than surrounding bone. A significant difference in elastic modulus and relative density between the titanium alloy and surrounding bone can cause significant stress transfer effects. Furthermore, the stress stimulation value near the implant in bone is lower than recommended for bone regeneration, leading to absorption of bone tissues around the implant, resulting in implant loosening and ultimately failure.

One potential consequence of such an effect is gradual weakening of the jawbone as the implant assumes a large portion of the load. Evaluation of implant geometric and mechanical properties and their effects is based on loading conditions, associated stresses, and patterns of implant and bone tissue deformation, considering the combined effect of different properties.

2. Materials and methods

Model A: implant with internal octagonal connection and matching platform, and a preformed abutment with screw. Model B: implant with internal hexagon connection and switching platform, and a milling wearable abutment with screw. Model C implant with internal conical-cylindrical connection and switching platform, and a cementable abutment with screw. The study was carried out using FEM and three study models were built. The parameters used for the construction of the models were as follows: to replicate the geometry of the components of each dental implant system (abutment, screw, and dental implant), preexisting plans were analysed from the implant manufacturing companies. The models were assembled and meshed using finite element software (SolidWorks 2022).

Chewing is a complex biomechanical process that involves the movement of the jaw when food is in the mouth, initiating the chewing cycle. Therefore, dental implants are exposed to a large number of loading cycles during their useful life. This causes mechanical wear of the material (fatigue phenomenon), which reduces its resistance, makes it susceptible to the formation of microcracks, and results in their propagation until failure occurs. The combination of axial and non-axial loading, termed mixed loading, simulates practical conditions where the actual applied force can be inclined with respect to the implant axis. In this finite element study, a frictional coefficient of 0.5 is assumed between the implant, abutment, and screw.

Table 1

Materials and mechanical properties

Material	**Young's Modulus (MPa)**	**Poisson's Ratio**	**Yield Strength (MPa)**
Cortical Bone	13.700	0.3	150
Cancellous Bone	1.370	0.3	130
Ti-6Al-4V	110.000	0.3	870

Table 2

Maximum von Mises stress and in all three study models

IMPLANT MODEL	**Maximum von Mises Stress (MPa)**		**Displacement (mm)**	
A	**Bone**	**Implant**	**Bone**	**Implant**
	40.5	135	0.010	0.1010
B	**Bone**	**Implant**	**Bone**	**Implant**
	51.49	187.2	0.00858	0.01
C	**Bone**	**Implant**	**Bone**	**Implant**
	59.45	293.3	0.01977	0.02668

A 3D solid-type mesh with tetrahedral elements based on curvature was used, which provided greater precision in the analysis of results due to its automatic creation of more elements in areas of greater curvature adapted to the circumferential shapes of the implants.
The Young's modulus, Poisson's rate and yield stress are shown in Table 1. The stress distribution was assessed using the von Mises stress through the comparison of normal, principal, and equivalent stresses.

3. Results

Axial load was applied on the surface of the abutment to analyse the stress distribution and determine the maximum stress values; the stress distribution was evaluated using von Mises stress. After applying an axial load, Model A showed a maximum von Mises stress value of 135 MPa (Table 2). Models B and C showed maximum von Mises stress values of 187.2 MPa and 293.3 MPa (Table 2); this stress was concentrated on the implant neck in all models (Figure 1-3).

von Mises stress **Displacement**

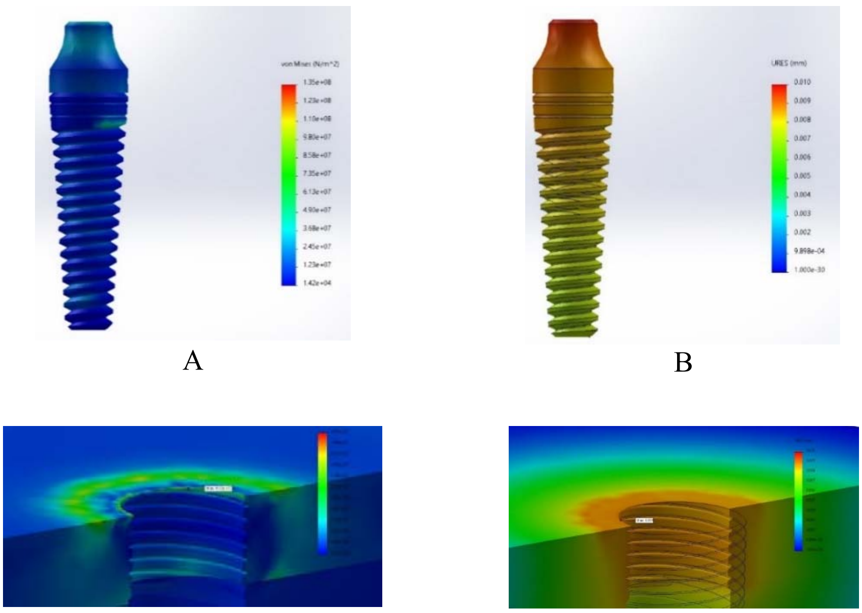

Figure 1. *Model A subjected to a 300 N axial load*

von Mises stress **Displacement**

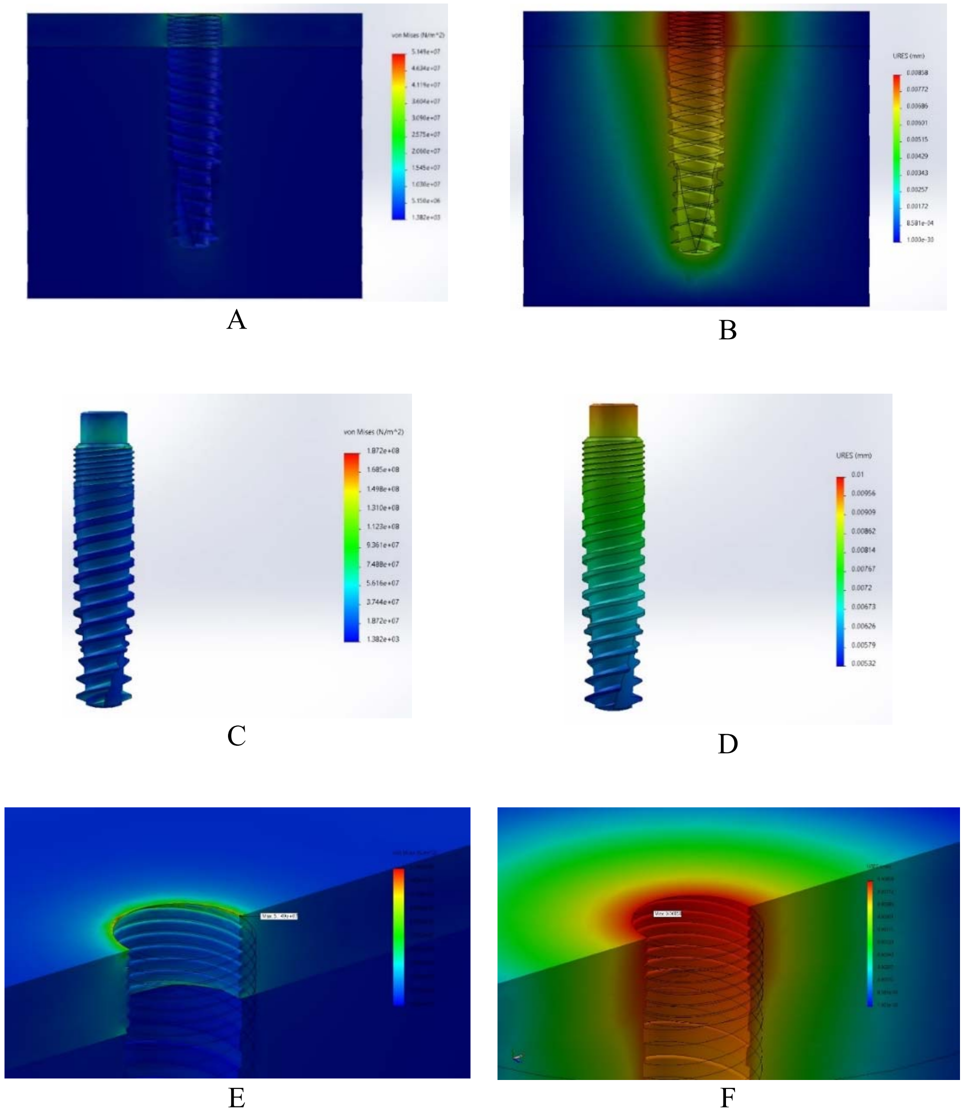

Figure 2. *Model B subjected to a 300 N axial load*

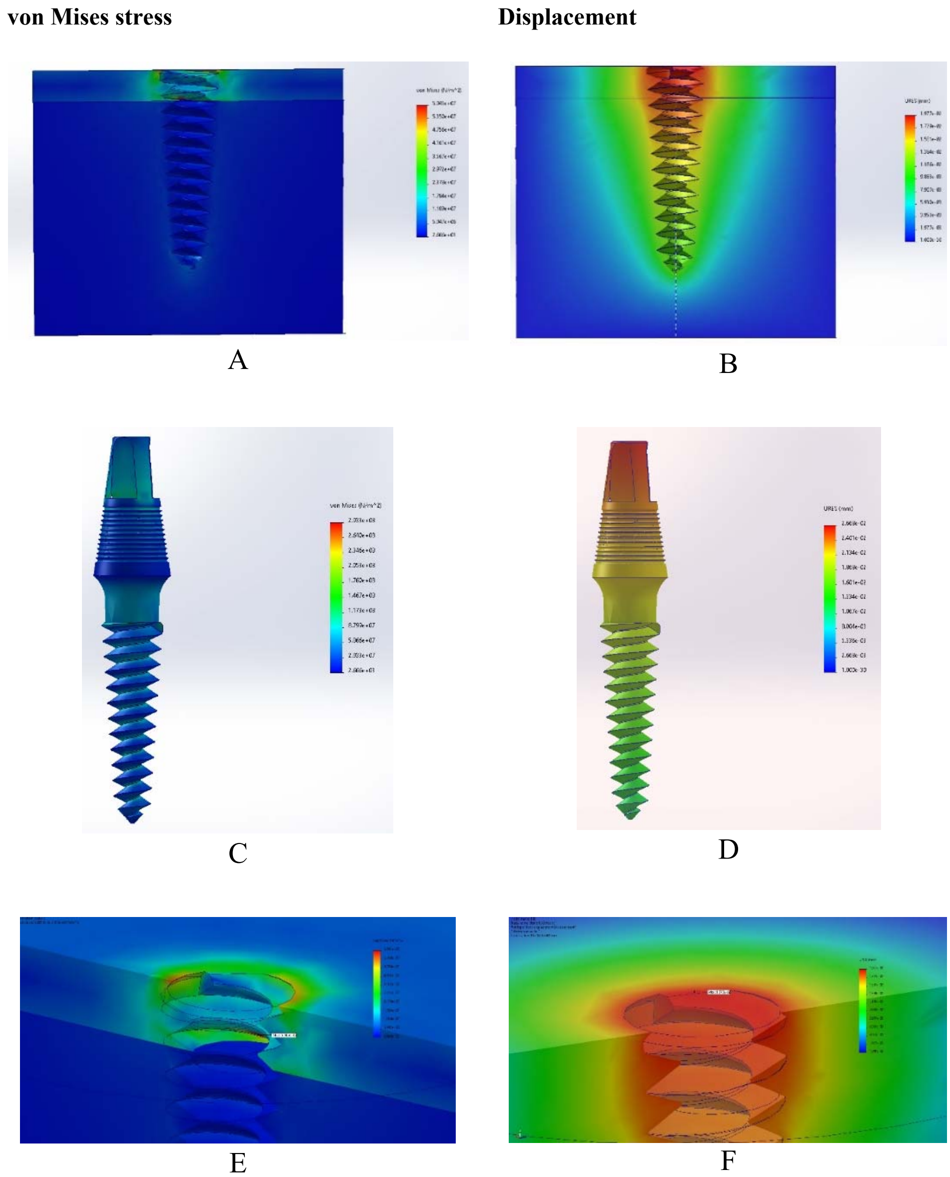

Figure 3. *Model C subjected to a 300 N axial load*

In dentistry, platform switching is a method used to preserve alveolar bone levels around dental implants, is whenever an abutment is used that is smaller in diameter than the implant platform. Platform switching can help prevent crestal bone loss, which is fundamental for the implant's long-term success and stability. The implant-abutment connection plays a crucial role in stress distribution. The reduction of stress at the implant-abutment connection may avoid some mechanical complications, such as abutment fracture, screw fracture, screw loosening, and augmented leakage at the implant-abutment connection.

We found that implants with conical connections showed lower stress than implants with internal hexagonal connections. The internal conical connection generated greater resistance to deformation and fracture. The stress concentration on the abutments is higher than on the implant. The highest stress values were formed on the abutment and on the upper part of the implant.

4. VIKOR METHOD IN DECISION SUPPORT

During the development process, we ranked different alternative solutions and the process of selecting the most suitable option: based on 7 criteria, we ranked the 3 alternatives with the VIKOR method. The models of the produced alternatives and the results of the finite element load simulations performed on them were collected and processed, and the alternatives were ranked using the VIKOR method applied in Excel. The results of the evaluation process are shown in Table 4.

Table 3

Criteria taken into account during the process of comparing alternatives and their priorities

Criteria	Importance
C1 cost	6
C2 deformation in bone	7
C3 deformation in implant	8
C4 maximum stress in bone	10
C5 operational lifespan	6
C6 maximum stress in implant	9
C7 repair request	5

Table 4

Determination of the ranking of the alternatives

Implant model	**Criteria**						
	C1	C2	C3	C4	C5	C6	C7
Model A	10	0.010	0.1010	40.5	100	135	100
Model B	7	0.00858	0.01	51.49	100	187.2	100
Model C	8	0.01977	0.02668	59.45	100	293.3	100
	0.0612	0.1836	0.1632	0.2040	0.1224	0.1836	0.0816
Ranking: Model A Model B Model C							

5. SUMMARY

Models with switching platforms with an internal hexagon or conical-cylindrical connection generate lower maximum stress values, the major areas of stress were concentrated on the implant-abutment interface and the surrounding cortical bone. The results of the simulations on different alternatives and the application of the VIKOR method, which establishes a ranking based on the evaluation criterion system, can be concluded that it effectively supports the development processes of dental implants.

REFERENCES

Albert, J., & Takács, Á. (2020). Application aspects of the VIKOR algorithm in material selection decisions. *GÉP, 71*(7-8), 65-68.

Albert, J., & Takacs, A. (2022). The VIKOR Algorithm in Material Decision Support. *DESIGN OF MACHINES AND STRUCTURES, 12*(2), 5-13. doi:https://doi.org/10.32972/dms.2022.008

Jahan, A., & Edwards, K. (2013). *Multi-criteria Decision Analysis for Supporting the Selection of Engineering Materials in Product Design.* Butterworth-Heinemann.

Koosha, S., Jalalian, E., Safari, S., & Zandrahimi, S. (2017). Effect of Abutment Angulation and Material on Stress and Strain Distributions in Premaxillary Bone: A

Three-Dimensional Finite Element Analysis. *Journal of Research in Dental and Maxillofacial Sciences, 2*(4), 1-8. doi:https://doi.org/10.29252/jrdms.2.4.1

Martinez-Mondragon, M., Urriolagoitia-Sosa, G., Romero-Ángeles, B., García-Laguna, M., Laguna-Canales, A., Pérez-Partida, J., . . . Urriolagoitia-Calderón, G. (2024). Biomechanical Fatigue Behavior of a Dental Implant Due to Chewing Forces: A Finite Element Analysis. *Materials, 17*(7), 1669. doi:https://doi.org/10.3390/ma17071669

Mbogori, M., Vaish, A., Vaishya, R., Haleem, A., & Javaid, M. (2022). Poly-Ether-Ether-Ketone (PEEK) in orthopaedic practice- A current concept review. *Journal of Orthopaedic Reports, 1*(1), 3-7. doi:https://doi.org/10.1016/j.jorep.2022.03.013

Opricovic, S. (1998). *Multicriteria Optimization of Civil Engineering Systems.* University of Belgrade. Belgrade: Faculty of Civil Engineering.

Shunmugasamy, V., Gupta, N., Pessoa, R., Janal, M., & Coelho, P. (2011). Influence of Clinically Relevant Factors on the Immediate Biomechanical Surrounding for a Series of Dental Implant Designs. *Journal of Biomechanical Engineering, 133*(3). doi:https://doi.org/10.1115/1.4003318

Design of Machines and Structures, Vol. 14, No. 1 (2024), pp. 84–94.
https://doi.org/10.32972/dms.2024.008

PROPOSAL OF PARAMETER CONTROL DESIGNATION SYSTEM OF ADDITIVELY MANUFACTURED PARTS

LEVENTE WOLAREK[1] – BÁLINT LEON SEREGI[2] – PÉTER FICZERE[3]

Budapest University of Technology and Economics,
Department of Railway Vehicles and Vehicle System Analysis,
1111, Budapest, Műegyetem rkp. 3
[1]wolarek.levente@edu.bme.hu, [2]seregibalint@edu.bme.hu, [3]ficzere.peter@kjk.bme.hu
[3]https://orcid.org/0000-0003-3207-5501

Abstract: As additive manufacturing is getting more and more widespread, the need for a system regarding the technical documentation is getting more required. The tremendous amount of manufacturing parameters makes the performance of the part hard to assess. Same parameters are used with different names and there is no common knowledge of how these parameters affect the part precisely. We can find a serious amount of research data and results, but only a small portion of them is able to be compared because of the different measuring techniques or similar investigation of parameters. To be more effective with the data gathering, a systematic way of recording these aspects is needed. In this article we propose a robust way of recording information on technical drawings of additively manufactured parts. We also discuss the difficulties and future opportunities implemented by this method.

Keywords: *additive manufacturing, standardization, technical drawing*

1. INTRODUCTION

The conventional subtractive technologies have a significant effect on the design philosophies knowing the limits of the used manufacturing devices. Additive manufacturing (AM) methods differ from this approach by adding successive layers of material on top of each other. The demand for 3D printing has increased significantly during the last decade by reaching the required level of efficiency (Thompson, et al., 2016). Economic factors also allowed the development of the technology, since the production time decreased. The early technologies were responsible for rapid prototyping, but the approach has widened towards manufacturing final products as well. The processes are much more robust, because

AM methods do not require such complex tooling as the traditional manufacturing, making it easier if the nature of the product changes. The various AM technologies are SLS (Selective Laser Sintering), FDM (Fused Deposition Modelling), SLA (Stereolithography) and FFF (Fused Filament Fabrication).
The major issues with AM methods are the lack of proper common knowledge of the effects of parameters (Bhardwaj, et al., 2019). The number of studies characterizing these methods increased over the past couple of years, but they usually focus on mechanical properties (Albert & Takács, 2023). Designing for life cycles is still in the early stages compared to the conventionally manufactured parts in terms of survival safety. The nature of the technology requires the overall review and the standardization of the manufacturing parameters. The mechanisms regarding the layered structure still have not been fully covered yet. The knowledge could be essential for engineers to make the best decisions possible in terms of part utilization (Seregi, 2023).
In today's engineering work, Computer-Aided Design (CAD) has become a fundamental part. With the advancement of CAD systems, 3D models can now carry an increasing amount of information, which may be sufficient for the precise manufacture of the part. Therefore, the relevance of 2D technical drawing is questionable, although practice does not necessarily reflect this (Ficzere & Győri, 2016). During manufacturing, companies and professionals still use these drawings as fundamental documents, forming the basis for the production of the final component. Additionally, certain product documentation and descriptions may only appear in 2D format. As 2D drawings continue to prove their significance an increasing number of manufacturing methods are becoming more widespread and accessible. However, for some manufacturing technologies, creating drawings with the appropriate structure is challenging due to the peculiarities of the technology itself. AM technologies fall into this category. Despite the growing prevalence of AM, current drawing notations and standards are no longer sufficient. Therefore, the development of a new supplementary notation system is necessary. This new system has to comply to the present standards, so the integration has to be done with caution and reason. It must be compatible with Geometric Dimensioning and Tolerancing (ISO 1101), title blocks, manufacturing instructions and operation plans.

2. STANDARDIZATION OF PARAMETERS

In order to control the manufacturing conditions, it is essential to appropriately define the parameters themselves. Specifying what each of the parameters signify and its corresponding impact a necessary first step. Some of the parameters are defined partially in already existing standards (ISO/ASTM 52900). The parameters must not only be accurately described but also addressed for each branch of related additive manufacturing technology.

In the scope of our investigation, we are initially focusing on the FFF and FDM, in summary form Material Extrusion (MEX) technologies. To establish a comprehensive framework and workflow, it is essential to specify the manufacturing parameters which have great influence on the final state of the workpiece. We can distinguish primary and secondary parameters whose classification defines the impact on other parameters and on the entire quality of the workpiece. Additionally, we have the capability to distinguish between global and local parameters, a characteristic applicable to all secondary and the majority of primary parameters as it can be seen in Figure 1. Some of these parameters are defined by the machine itself and others can only be adjusted in the slicer settings (Kuznetsov, Tavitov, Urzhumtsev, Mikhalin, & Moiseev, 2019).

	Technical drawing	Operation plan
Printer parameters	Nozzle diameter Colour Model material Support material	Hotend temp Bed temp Chamber temp Print speed
Slicer parameters	Layer height Wall width Top/bottom layer width Infill pattern Infill density Orientation	Support control Local min wall width Local layer height Hole ovality (support/adaptive LH) Raster angle (infill, top/bot layer) Line width Ironing
Post-process	Surface finish Technology allowance (for milling or grinding) Insert/bushing placement and type Thread taping	

Figure 1. *Primary and secondary printing parameters sorted by parameters source and place of definition*

3. DOCUMENTATION

Not all parameters can be properly specified on the technical drawing, therefore, the manufacturing documentation needs to be supplemented with an operation plan, similar to the one used in machining. With this document, parameters that would require the modification of the views for their designation or those whose definition necessitates a more detailed textual explanation, can be precisely defined in a designated space created for this purpose. Only one literature regarding the drawing symbols for additive parts was found (Simion & Arion, 2016). The authors considered just a fraction of the parameters available in FFF processes, but this paper was the only reference for this work.

Technical drawing

Global parameters

In the technical drawing, we aim to designate global parameters using a table, as they significantly constrain several other parameters and the outcome of the workpiece. These are the variables most frequently adjusted. The parameters listed in the table are influenced by the first parameter, which is the type of AM technology. In this example, we are seeking solutions for FFF and FDM technologies, so their primary parameters are included in Table 1. The table serves a similar function to the tooth profile table found in workshop drawings of gears. While the teeth are not precisely drawn and dimensioned, they can be manufactured without issues because the table contains all the necessary data. In our case, this would result in a very long table, so we only include the primary parameters that are most frequently varied.

Table 1.
Primary parameters on the drawing

Additive manufacturing parameters		
Technology	FFF	-
Nozzle diameter		mm
Model material		-
Support material		-
Colour		-
Layer height		mm
Shell thickness		mm
Line width		mm
Infill pattern		-
Infill density		%

As it is presented in Figure 1, the wall, bottom and top layer widths are considered differently, but in the parameter table we merged them into the parameter called shell thickness. The reason for not specifically marking these is that a uniform thickness is expected on all cladding surfaces unless a different value is locally specified. Therefore, individual markings for these are not shown. Differentiating the wall thickness from the top/bottom thickness is presented in this work below. If there is any parameter that needs to be specified, a text like "Local parameters marked on view or operation plan!" could refer to the operation plan which contains the parameters.

Orientation

One of the first parameters that has the greatest influence on the performance of a part is the printing direction or orientation. To control the printing direction, we propose an orientation specification with a reference arrow used next to a view (Figure 2). The arrow has to point to the Z direction which is the slicing direction of all common printers. This sign is easily understandable and catches the eye on the drawing making it hard to miss. If there is a crowded drawing with multiple views on it, a text above the title block saying, "Manufacturing direction marked on view!" gives robust feedback.

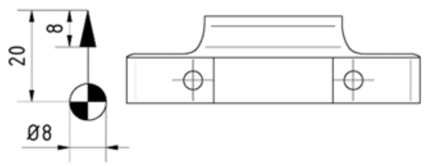

Figure 2. *Symbol to designate the orientation of the part*

Local minimum wall width

In certain cases, it is locally necessary to increase the number of walls. This can be attributed to technological allowance, drilling threads or threaded insert installing during post-processing, or simply to enhance the surface stiffness of a specific geometric feature. We propose to control the required wall width by extending the dimension of feature with a special symbol that can be seen on Figure 3. It is crucial to understand that the symbol represents the minimum width of walls required to a feature for special purposes. In Material Extrusion (MEX) technologies width of wall is constrained by the diameter of the nozzle and controlled with the material feed rate (extrusion rate measured in mm^3/s), which results in the line width parameter. As presented above, in Table 1 the nozzle diameter is defined, which combined with the line width gives the wall width sizes achievable (Kim, et al., 2022). Some slicers are capable of varying the line width to follow the contour of a section as close as possible, but this specific control option is not common.

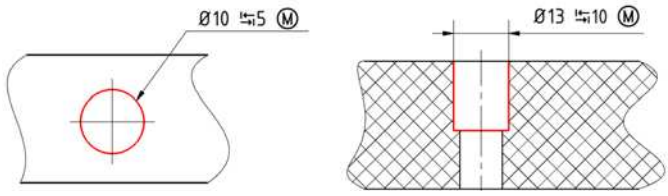

Figure 3. *Callout of min wall width (the red contour is optional on the technical drawing, but mandatory on the figure of the operation plan*

In Figure 3 we can see a circled letter M, which is a Geometric Dimensioning and Tolerancing (GD&T) specification meaning Maximum Material Condition (MMC). In this situation, used with the minimum wall width sign, we would like to emphasise that the number given is a minimum, meaning if it is necessary (because of the nozzle diameter or line width constraint) more walls have to be added to achieve the minimum desired value. This becomes particularly crucial when the intention is to tap a thread into a hole as post-processing. Insufficient wall thickness not only compromises the strength of the thread but may lead to breakage during the drilling process.
On the operation plan the minimum wall thickness can also be defined just by marking the feature and adding the parameter in the corresponding cell. It is up to the user to use the custom width and MMC mark or just marking the feature with a letter. (See the examples in Figure 4.)

Operation plan

Minimum wall width

As presented above we can define local minimum wall width on the technical drawing and the operation plan. To avoid the crowded drawing it seems to be a better solution to define these local parameters in the operation plan. This document also provides extra data entries, like a description where the reason of the specified parameter can be seen explained. (See in Figure 7.)

Support control

Specifying all the support parameters could be a separate document because of the number of subparameters it consists of. In this system we are trying to define only the parameters, which are crucial for the adequate manufacturing of the workpiece and not going to the lowest class of parameters only if necessary. The most commonly changed parameters of the support (besides the supported surfaces) are type, Z gap, support density, support number of walls, support pattern, interface density, interface pattern, interface height, XY distance from model, overhang angle. There can be situations when too much support is prohibited or have to be avoid. Prohibiting a support on a surface can be marked in a way showed in Figure 5. If a surface (for example a laying hole) needs to be supported, but we do not want to use too much support (starting from the build plate), support dead zones can be specified.

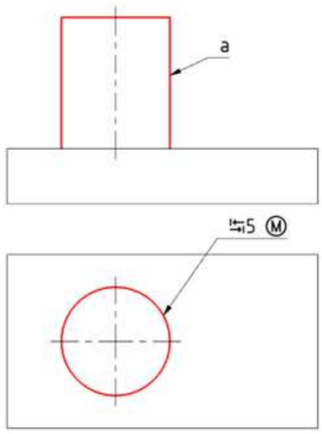

Figure 4. *Callout of min wall width without the size of the feature or parameter*

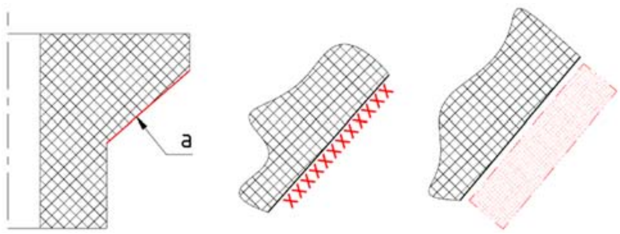

Figure 5. *Support controlled surfaces: marked with letter (left), marked with prohibition (middle) and marked with dead zone (right)*

Local layer height

The same way we mark the local wall width, we can designate the local layer height. In case of defining this parameter, two options have to be differentiated. We can set local layer heights section-wise through the whole part, or we can set it feature-wise (See Figure 6.). The goal of the two options is the same, the height difference between the height steps has to be considered. Having a larger height layer on the top of a much smaller one results a bad interlayer adhesion and porosity (Naresh, Raju, & Parveen, 2023). This is the same constrain we have to consider in case of the adaptive layer height.

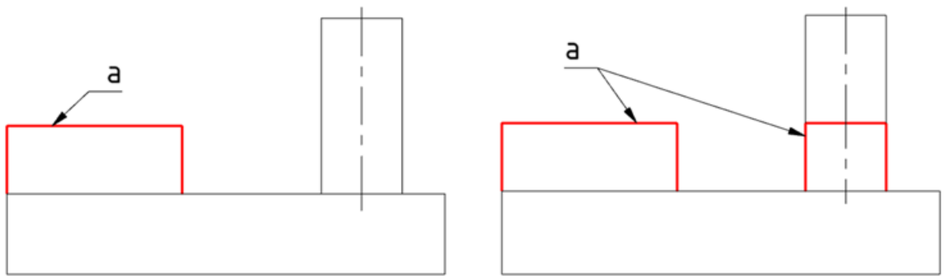

***Figure 6.** The two options of variating the local layer height: feature-wise (left) and section-wise (right)*

In the presented system, a precise understanding of parameters and their interrelationship is fundamental. This holds true especially in the context of GD&T, where it becomes a necessary condition, as it is easy to specify tolerances that contradict each other. Therefore, a thorough knowledge of manufacturing parameters is a key consideration for a given technology. A straightforward example of this is specifying a layer height that the nozzle, due to its diameter and the hot end, cannot physically provide.

The provided table of the operation plan (Figure 7) functions as a collection of all local parameters. This way it is easier to detect contradicting parameter changes and gives a channel of information between the designer and the person who handles the slicer software. This version is work in progress, as we also need to collect parameters which the other types of AM technologies have. There can be some parameters which are also hard to define even in an operation plan.

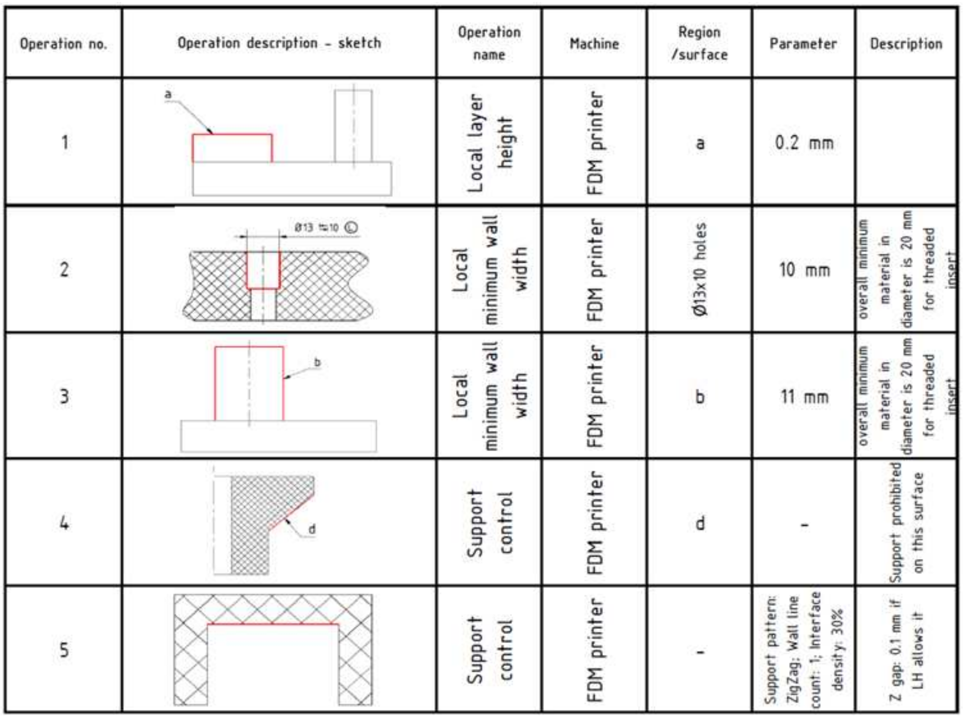

Operation no.	Operation description - sketch	Operation name	Machine	Region /surface	Parameter	Description
1	a	Local layer height	FDM printer	a	0.2 mm	
2	Ø13 ↧10 Ⓒ	Local minimum wall width	FDM printer	Ø13x10 holes	10 mm	overall minimum material in diameter is 20 mm for threaded insert
3	b	Local minimum wall width	FDM printer	b	11 mm	overall minimum material in diameter is 20 mm for threaded insert
4	d	Support control	FDM printer	d	-	Support prohibited on this surface
5		Support control	FDM printer	-	Support pattern: ZigZag; Wall line count: 1; Interface density: 30%	Z gap: 0.1 mm if LH allows it

Figure 7. *Examples of operation plan entries*

Additional elements

There are more parameters that we have not covered yet, but we collected more in Figure 1. Some of these parameters are already mentioned in connection with others, but some of them are left out totally. One of them is the raster angle. It is necessary to be mentioned because of its importance regarding the structural strength of the workpiece (Srinivasan Ganesh Iyer & Keles, 2022), (Sangaletti, Aranda, Távara, & García, 2024). We had difficulties finding a correct way of defining this angle and kindly ask the reader to provide their ideas if they have one. The latest idea was defining an angle on a view with a datum in the operation plan. If the orientation is fixed, then we can only move the part on build plate in the XY plane and rotate it around the Z axis. By rotating it, the orientation of the raster angle changes relative to the part, so we need a way of defining it on one of the part views in a robust way. As we could not provide a failsafe idea, we did not provide any graphics for this parameter.

Another problem is the dimensioning of the drawing. Using AM enables to create and design complex shapes, which are hard to fully define dimensionally. In case of the lattice structures a single unit parameter can be defined and the volume it fills, but with shapes that are generated with generative design or topology optimization, the freeform geometries cannot be described (Li, Yang, Bian, Zhang, & Wang, 2023). Even a human made geometry which is fitted for AM can be so complex, that it would take many views and make the drawing crowded and hard to read. Despite the problem, it would be crucial to establish a drawing or sizing method that allows for the definition of the entire workpiece without making the drawing too complicated.

4. SUMMARY

In this work, we addressed the manufacturing and technical documentation challenges arising from AM. Exploring the topic, we presented numerous proposals that could serve as guidance. Initially, we dug into parameters related to FFF and FDM technologies, classifying and organizing parameters. Subsequently, we recommended a notation system for the clear and understandable definition of these parameters. We plan to expand this system to other AM technologies in the future. At the beginning of the research, we took that into account there are already standards related to AM, but we did not encounter practical ones covering specific issues except for a paper (Simion & Arion, 2016) similar to our work.

REFERENCES

Albert, J., & Takács, Á. (2023). Additív gyártás biomimetikai megközelítéssel, GÉP 74 : 4 pp. 9-11. , 3 p.

Bhardwaj, A., Jones, S., Kalantar, N., Pei, Z., Vickers, J., Wangler, T., . . . Zou, N. (2019). Additive Manufacturing Processes for Infrastructure Construction: A Review. *Journal of Manufacturing Science and Engineering, 141*(9). doi:https://doi.org/10.1115/1.4044106

Ficzere, P., & Győri, M. (2016). A jelképes ábrázolásból adódó problémák vizsgálata gyárthatósági szempontból 2D-s ábrázolás és 3D-s testmodellek használata esetén. *GÉP, 67*(5-6), 70-73.

Kim, S., Andreu, A., Kim, I., Kim, J.-H., Lee, J., & Yoon, Y.-J. (2022). Continuously varied infill pattern (ConVIP): improvement of mechanical properties and printing speed of fused filament fabrication (FFF) 3D printing. *Journal of Materials Research and Technology, 18*, 1055-1069. doi:https://doi.org/10.1016/j.jmrt.2022.02.133

Kuznetsov, V., Tavitov, A., Urzhumtsev, O., Mikhalin, M., & Moiseev, A. (2019). Hardware Factors Influencing Strength of Parts Obtained by Fused Filament Fabrication. *Polymers, 11*(11), 1870. doi:https://doi.org/10.3390/polym11111870

Li, P., Yang, F., Bian, Y., Zhang, S., & Wang, L. (2023). Design of lattice materials with isotropic stiffness through combination of two complementary cubic lattice configurations. *Acta Mechanica, 234*, 1843-1856. doi:https://doi.org/10.1007/s00707-023-03480-y

Naresh, D., Raju, R., & Parveen, S. (2023). Design and development of alternate layer printing method to reduce the porosity in FDM printing process. *International Journal on Interactive Design and Manufacturing (IJIDeM)*. doi:https://doi.org/10.1007/s12008-023-01624-x

Sangaletti, S., Aranda, M., Távara, L., & García, I. (2024). Effect of stacking direction and raster angle on the fracture properties of Onyx 3D printed components: A mesoscale analysis. *Theoretical and Applied Fracture Mechanics, 129*, 104228. doi:https://doi.org/10.1016/j.tafmec.2023.104228

Seregi, B. (2023). Gyártási paraméterek dinamikai hatásainak vizsgálata additív módon gyártott darabokon.

Simion, I., & Arion, A. (2016). Dimensioning Rules for 3D Printed Parts Using Additive Technologies (FDM). *University Politechnica of Bucharest Scientific Bulletin, Series D, 78*(2), 79-92.

Srinivasan Ganesh Iyer, S., & Keles, O. (2022). Effect of raster angle on mechanical properties of 3D printed short carbon fiber reinforced acrylonitrile butadiene styrene. *Composites Communications, 32*, 101163. doi:https://doi.org/10.1016/j.coco.2022.101163

Thompson, M., Moroni, G., Vaneker, T., Fadel, G., Campbell, R., Gibson, I., . . . Martina, F. (2016). Design for Additive Manufacturing: Trends, opportunities, considerations, and constraints. *CIRP Annals, 65*(2), 737-760. doi:https://doi.org/10.1016/j.cirp.2016.05.004